On the consistency of methane isotopologue retrievals using TCCON and multiple spectroscopic databases.

Edward Malina[1], Ben Veihelmann[1], Dietrich G. Feist[2,3,4], and Isamu Morino[5]

[1]Earth and Mission Science Division, ESA/ESTEC, Keplerlaan 1, Noordwijk, the Netherlands.
[2]Lehrstuhl für Physik der Atmosphäre, Ludwig-Maximilians-Universität München, Munich, Germany
[3]Deutsches Zentrum für Luft- und Raumfahrt, Institut für Physik der Atmosphäre, Oberpfaffenhofen, Germany.
[4]Max Planck Institute for Biogeochemistry, Jena, Germany.
[5]Satellite Remote Sensing Section and Satellite Observation Center, Center for Global Environmental Research, National Institute for Environmental Studies, Onogawa 15-2, Tsukuba, Japan.

Correspondence: Edward Malina (edward.malina.13@alumni.ucl.ac.uk)

Abstract. The next and current generation of methane retrieving satellites are reliant on the Total Carbon Column Observing Network (TCCON) for validation, and understanding the biases between satellite and TCCON methane retrievals is as important as when TCCON started in 2010. In this study we highlight possible biases between different methane products by assessing the retrievals of the two main methane isotopologues $^{12}CH_4$ and $^{13}CH_4$. For this study we use measurements from two TCCON sites, namely Ascension Island in the Atlantic Ocean and Tsukuba, Japan, with different spectroscopic databases.

Using the TCCON GGG2014 retrieval environment, retrievals are performed using four separate spectroscopic databases and a set of spectral fit windows. Databases used include the TCCON spectroscopic database; the HIgh-resolution TRANsmission molecular absorption database 2016 (HITRAN2016); the Gestion et Etude des Informations Spectroscopiques Atmosphériques 2015 (GEISA2015) database; and the ESA Scientific Exploitation of Operational Missions - Improved Atmospheric Spectroscopy Databases (SEOM-IAS) database. We report the biases between the retrievals using standard TCCON methane windows, and specific windows based on the sensitivity of the instruments TROPOspheric Ozone Monitoring (TROPOMI) present on Copernicus Sentinel-5P (S5P) and the future Sentinel 5 (S5) mission present on MetOp-Second Generation satellite. We assess the biases in retrieving methane isotopologues using these different spectral windows and different spectroscopic databases. The sensitivity of these biases (across windows and databases) to locally changing atmospheric conditions, and uncertainties in the a priori and parameter information, specifically pressure, temperature, methane and water vapour profiles are also quantified.

We find significant biases between retrievals calculated using differing spectroscopic databases and windows for both methane isotopologues, with up to a 3% bias between $^{12}CH_4$ retrievals. These biases depend on the conditions under which they were captured, with specific windows showing larger biases at higher Solar Zenith Angles (SZA). In addition, the sensitivity to a priori assumptions are shown to be significant and we find the biases between spectroscopic databases change depending on the introduced error, with methane profile shape and water vapour profile uncertainty causing significant differences. Retrievals using the S5P/TROPOMI spectral range show the results with the least variation between spectroscopic databases, and we therefore recommend that this band should be considered in future TCCON methane retrievals.

1 Introduction

Methane is widely acknowledged to have a significant impact on the global climate (IPCC, 2014), but the processes via which it enters and is removed from the atmosphere are still not as well understood as is the case for carbon dioxide; with bottom up estimations of the global methane budget not agreeing with top down estimations (Kirschke et al., 2013; Saunois et al., 2019). This disconnect is one of many reasons which has led to the development of multiple satellite missions, with the aim of improving the knowledge of the global methane budget.

The recent launch of the S5P satellite, with the TROPOMI instrument (Veefkind et al., 2012), and the future S5 mission with its Ultra-Violet Near infrared Shortwave infrared (UVNS) instrument (Ingmann et al., 2012), represent a significant advancement in space-based Greenhouse Gas (GHG) remote sensing.

TROPOMI and UVNS exploit the 4190 – 4340 cm^{-1} spectral range, which has not been explored in detail from previous space-based instruments for methane retrievals. The Scanning Imaging Absorption spectrometer for Atmospheric CartograpHY (SCIAMACHY) (Bovensmann et al., 1999) onboard the ENVIronmental SATellite (ENVISAT) was sensitive to this spectral range, but was plagued with detector issues (ice build-up). The Measurements Of Pollution In The Troposphere (MOPITT) (Drummond and Mand, 1996) is also sensitive to this spectral range, but is also affected by technical issues and has never successfully retrieved methane in this spectral window. In addition, the wide spectral sensitivity of the limb viewing Canadian Atmospheric Chemistry Experiment (ACE)- Fourier Transform Spectrometer (FTS) (Bernath et al., 2005) includes this spectral window, but again the methane products of ACE-FTS do not include retrievals in this window. S5P/TROPOMI and S5/UVNS will therefore be relying on spectroscopic parameters for which only limited experience is available in their application to space based methane retrieval instruments (Checa-Garcia et al., 2015; Galli et al., 2012). This extends to TCCON, which although sensitive to this spectral range, has primarily provided its methane abundances retrieved from the 6000 cm^{-1} spectral range, allowing for direct comparisons with SCIAMACHY .

In this study, we make retrievals of the two main methane isotopologues using the TCCON GGG2014 (Toon, 2015) retrieval environment. Spectra are taken from two different TCCON sites and over multiple seasons, assess the impact of varying atmospheric conditions. We assess the differences in abundances of the isotopologues, the retrieval errors and the quality of the fits when retrieved from standard TCCON spectral windows, and methane spectral windows in the TROPOMI/UVNS spectral range. We also quantify the variations in retrieval abundances when using four separate spectroscopic databases, and the application of non-Voigt line broadening shapes. The sensitivity of the retrievals to errors introduced into the a priori and parameter profiles are assessed, allowing for the assessment of how differing windows and spectroscopic databases are sensitive to these errors.

TCCON is a global network of 27 ground based Fourier Transform Spectrometers (FTS) (Wunch et al., 2010), with the primary aim of providing reference total column (an weighted average value for a nadir viewing profile) abundances of numerous atmospheric species calibrated against aircraft profiles (Wunch et al., 2010, 2011), including methane, for validation and

cross-calibration purposes. TCCON operates in a wide spectral range (4000 – 15000 cm^{-1}) and records direct solar spectra. TCCON is currently one of the key sources of reference data for the validation of satellite-based GHG retrievals (Yoshida et al., 2011; Crisp et al., 2012; Parker et al., 2015). Examples include the Orbiting Carbon Observatory (OCO)-2 and the Greenhouse Gases Observing Satellite (GOSAT) (Kuze et al., 2009). TCCON instruments have both high spectral resolution (0.02 cm^{-1}), and high Signal to Noise Ratios (SNR) due to direct solar viewing geometry, thus making TCCON measurements higher quality than satellite measurements. TCCON and TROPOMI/UVNS both have overlapping spectral windows in the Shortwave Infrared (SWIR) methane absorption regions, highlighted in Table 1.

Table 1. Methane SWIR windows commonality between S5P/S5 and TCCON

Methane window	S5P/TROPOMI	S5/UVNS	TCCON
5970-6289 cm^{-1}	N	Y	Y
4190-4340 cm^{-1}	Y	Y	Y

When validating methane products from TROPOMI and UVNS, retrieval products using the 4190 – 4340 cm^{-1} window, will be compared with TCCON methane products generating using the standard TCCON windows (Table 2). Therefore potential biases associated with the choice of fit windows needs to be quantified and understood. Indeed, if the 4190 – 4340 cm^{-1} window proves to be accurate/stable, then there is justification to integrate TCCON retrievals from this window into future TCCON retrieval products. Numerous algorithms will be used to provide methane data products from TROPOMI/UVNS (Hu et al., 2016; Schneising et al., 2019), all of which will may use differing spectroscopic databases and are therefore subject to differing biases. The high SNR and high spectral resolution makes TCCON data an excellent resource to perform retrievals of methane isotopologues, and assess any potential variations due to differences in the spectroscopic databases, building on examples of similar past studies (Checa-Garcia et al., 2015; Galli et al., 2012). By investigating the biases present in TCCON observations made at several sites, we can infer some of the potential spectroscopic related biases in satellite retrievals and their dependencies on temperature and pressure. Our findings will inform as to the potential source of biases and are relevant to ongoing TROPOMI validation, and future S5/UVNS validation. We also make recommendations on spectral windows and databases for future methane retrievals.

TCCON methane products are the result of a standardised process where a weighted average of three retrieved values from three TCCON fit windows (described in Table 2 below) is reported. Assessments of the biases present in between these windows, with respect to the spectroscopic databases may help inform the future of TCCON methane products.

In addition to assessing the window and spectroscopic source biases for the two main methane isotopologues, the opportunity is taken to calculate the δ^{13}C metric which is a ratio of these isopologues (see Eq. 2). This is a metric which has been used in numerous studies globally to differentiate methane source types (Fisher et al., 2017; Nisbet et al., 2016; Rigby et al., 2017; Rella et al., 2015), e.g. industrial or wetlands. Calculating total column values of this metric would be highly beneficial for understanding the global methane budget, but is unlikely to be achievable with TCCON with an accuracy that would be sufficient for that purpose. However, calculation of δ^{13}C with TCCON will allow for an assessment of how far current

technology is from making a useful total column assessment. Calculation of the δ^{13}C metric requires the concentration of the two main methane isotopologues $^{12}CH_4$ and $^{13}CH_4$, which make up roughly 98% and 1.1% of global atmospheric methane respectively. Almost all measurements of this metric are limited to in situ studies or airborne flask measurements, which although highly accurate, by their nature are spatially limited. Some effort has gone into satellite based retrievals of this metric (Buzan et al., 2016; Weidmann et al., 2017; Malina et al., 2018, 2019), but the results of these studies show this to be a challenging task. Therefore the calculation of the δ^{13}C metric is a target of secondary importance in this study.

This paper is structured as follows, section 2 outlines the methods used in this study, including details about the TCCON sites and spectra used, as well as the retrieval method. Information about the spectroscopic databases used in this study are also given. The results of this study are shown in section 3. Section 4 outlines an assessment of the sensitivity of the retrievals to introduced errors in the a priori data and local condition variability. Section 5 discusses the results shown in sections 3 and 4, and conclusions are shown in section 6.

2 Methods, tools, datasets and requirements

2.1 TCCON spectra and tools

We use TCCON spectra from two different sites, firstly the Ascension Island site, found in the middle of the Atlantic Ocean near the equator. The second site is the Tsukuba site, near Tokyo in Japan, and at a higher latitude than Ascension Island. Ascension Island has an arid climate with a little precipitation, which remains largely constant through the year and does not have designated seasons but is subject to some variation. Tsukuba is subject to seasonal effects, with hot wet summers and cold dry winters, these two sites represent a wide range of atmospheric conditions. The Tsukuba spectra are generally captured in a narrow spread of SZAs, typically 35°<SZA<60°; Ascension Island spectra are captured under a much wider range of SZA, typically 10°<SZA<90°. This means that there will be larger variations in SNR for Ascension Island than Tsukuba, therefore leading to higher levels of radiometric noise and an increase in the random error, which could be significant for $^{13}CH_4$ retrievals.

In this study we use the GGG2014 environment which includes the GFIT retrieval algorithm (Wunch et al., 2010), the standard algorithm used by the TCCON sites for processing and distributing trace gas column abundances. GFIT is summarised briefly here; GFIT employs a nonlinear least-squares fitting scheme. A forward model (radiative transfer model which simulates radiation transfer through an atmosphere or a body of gas) is used to calculate synthetic irradiance spectra based on a set of parameters known as state vector elements (typically trace gas concentrations) and model parameters (e.g. temperature and pressure profiles). This synthetic irradiance spectra is then fit to the measured irradiance spectrum by adjusting the state vector elements to provide a final result, normally a trace gas abundance. In the case of GFIT the state vector includes the following.

- first target gas scaling factor (desired output).
- interfering gas scaling factor.
- continuum level of the irradiance spectrum.

- continuum tilt
- continuum curvature
- frequency shift
- zero level offset
- solar scaling (differences in shifts of atmospheric and solar lines)
- fit channel fringes

Note that all of the above are not routinely included in the state vector, for example the continuum curvature especially is not commonly included in the state vector. This option is designed to remove instrument features, but may also attempt to remove other effects due to the spectroscopic database, as noted in the TCCON wiki (TCCON, 2020). GFIT assumes a fixed profile shape for each trace gas, and the sub-column amount for each altitude/pressure level are not independently scaled. Unlike in most satellite retrieval algorithms, aerosol and albedo terms are not included in the state vector, this is because TCCON operates in direct solar viewing, where scattering is considered unimportant and surface terms are not necessary. The retrieved trace gas column is calculated by multiplying scaling factors from the retrieved state vector by the a priori vertical column abundances. Dry air Mole Fractions (DMF) are calculated by dividing the scaled trace gas column with the total column O_2, retrieved from a wide window in the 7885 cm^{-1} spectral range multiplied by the volume mixing ratio of O_2 0.2095. DMF gas concentrations identify retrieved concentration as mole fractions, as opposed to absolute concentrations, all retrieved $^{12}CH_4$ and $^{13}CH_4$ concentrations are referred to as DMF values.

Because of the high spectral resolution of the TCCON instruments (0.02 cm^{-1}), most spectral lines are resolved, radiative transfer calculations are performed on a line-by-line basis. GGG includes a spectroscopic database in its environment, which is similar to other more widely adopted databases (see below). TCCON has a standard set of spectral windows for methane retrievals, all of which are in the 6000 cm^{-1} methane absorption window range. In this study we include the TROPOMI/UVNS SWIR spectral windows (4190-4340 cm^{-1}). This window along with a description of all of the windows considered in this study are described in Table 2 below.

Table 2. Spectral windows used in study.

Window	Window spectral range (cm^{-1})	Target species	Background species	Window source
1	4190-4340	$^{12}CH_4$	$^{13}CH_4$, CO_2, H_2O, HDO, CO, HF, N_2O, O_3	Sentinel 5 baseline
2	5880-5996	$^{12}CH_4$	$^{13}CH_4$, CO_2, H_2O, N_2O	TCCON standard
3	5996.45-6007.55	$^{12}CH_4$	$^{13}CH_4$, CO_2, H_2O, N_2O, HDO	TCCON standard
4	6007-6145	$^{12}CH_4$	$^{13}CH_4$, CO_2, H_2O, N_2O, HDO	TCCON standard
5	4190-4340	$^{13}CH_4$	$^{12}CH_4$, CO_2, H_2O, HDO, CO, HF, N_2O, O_3	Sentinel 5 baseline
6	6007-6145	$^{13}CH_4$	$^{12}CH_4$, CO_2, H_2O, N_2O, HDO	TCCON standard

Windows 2-4 are standard TCCON methane retrieval windows which in this study are used for $^{12}CH_4$, and windows 1 is based on the TROPOMI spectral window (Galli et al., 2012; Hu et al., 2016), given that no standard windows exist in this spectral window for TCCON. Windows 5 and 6 are repeats of windows 1 and 4, but with $^{13}CH_4$ as the target.

2.1.1 Spectroscopic Databases

The introduction of $^{13}CH_4$ into spectroscopic databases in the TROPOMI spectral region is relatively recent, and in the case of HITRAN, was only introduced in the 2012 release. Indeed Gordon et al. (2017) reports that numerous new $^{13}CH_4$ lines were introduced into the latest HITRAN2016 release, this implies that the spectroscopic parameters of $^{13}CH_4$ in this region is not yet settled. A review of the documents released with numerous spectroscopic databases (Gordon et al., 2017; Jacquinet-Husson et al., 2016; Birk et al., 2017) suggest that $^{13}CH_4$ lines are not all sourced from the same laboratory studies. We therefore decided to compare methane isotopologue retrieval from four separate spectroscopic databases, which are as follows: 1) the database included with GGG2014 (Toon, 2015), which currently assumes a Voigt line shape for all lines. 2) HITRAN2016, HITRAN is a well-established spectroscopic database that has been used in numerous satellite based studies previously (Galli et al., 2012). The current release HITRAN2016 (Gordon et al., 2017) has been revised from the previous release (HITRAN2012) in terms of methane, with new lines and parameters included for both of the main isotopologues. HITRAN2016 does include the additional parameters required to model non-Voigt lines shapes, however the current version does not include these parameters for methane (at the time of writing). 3) The GEISA2015 database (Jacquinet-Husson et al., 2016) is another spectroscopic database, similar in design and goals to the HITRAN databases. The GEISA database does not currently include non-Voigt line shape parameters. 4) SEOM-IAS (Birk et al., 2017), specifically developed for the TROPOMI spectral window and designed around non-Voigt atmospheric line shape profiles. This database only has data within the 4190-4340 cm^{-1} spectral range, and can therefore only contribute to windows 1 and 5 of this study.

Some work has been performed previously comparing spectroscopic databases e.g. (Jacquinet-Husson et al., 2016; Armante et al., 2016), but this study is the first case with respect to the TROPOMI spectral window with TCCON.

2.1.2 Voigt vs non-Voigt line shape profiles

Ngo et al. (2013) states that the standard Voigt profiles used for spectral line broadening may be inadequate for trace gas retrievals (based on laboratory studies), which can lead to errors larger than instrument precision requirements. In order to calculate more accurate line shapes for remote sensing purposes, numerous models have been proposed. In this paper we use the quadratic Speed Dependent Hard Collision (qSDHC) model (Ngo et al., 2013; Tran et al., 2013). This model includes additional parameters based on speed dependence of collisional broadening and velocity changes of molecules due to collisions, on top of the standard parameters of pressure-induced air broadening, and pressure induced line shift. Note that only the SEOM-IAS database use these additional parameters, the remaining spectroscopic databases do not include these parameters for methane at the time of this paper. We use the FORTRAN routines provided with Ngo et al. (2013) to implement the qSDHC model into the GFIT algorithm, modified to include first order Rosenkranz line mixing effects. Mendonca et al. (2017) report that incorporating speed dependent and line mixing has a significant effect on calculated methane columns when compared against

assuming Voigt dependency. They find a 1.1% difference in total methane column abundances from 131,124 spectra. The implication being that it is important to account for the additional physical parameters included in non-Voigt models, when retrieving methane.

2.2 Metrics

Our main assessment metrics in this study are as follows.

- Averaging Kernels (AK): the AKs capture the sensitivity of the retrieved state vector to the truth, and is defined as $\mathbf{A} = \partial\hat{\mathbf{x}}/\partial\mathbf{x}$, where $\hat{\mathbf{x}}$ is the retrieved state vector and $\mathbf{x}$ is the truth. AKs are typically used in satellite and ground-based remote sensing to characterise the vertical sensitivity profile of a retrieval.
- Transmission spectra.
  - Root Mean Square Error (RMSE) of the residual between the calculated transmission spectra, and the TCCON measurement transmission spectra, expressed as the RMSE.
  - The quality of the fit, expressed via the χ^2 test, quantitatively defined as:

$$\chi^2 = \sum_i [\mathbf{y_{measured}} - \mathbf{y_{calculated}}]^2. \quad (1)$$

    Where $\mathbf{y_{measured}}$ refers to the measured TCCON spectrum, and $\mathbf{y_{calculated}}$ is the synthetic spectrum calculated by the forward model.
- Retrieved values.
  - Standard deviation of the DMF for each window (σ_{window}).
  - Standard deviation of the DMF between all windows for a specific database ($\sigma_{inter-window}$)
  - Bias of the retrieved mean of the DMF for each window against the retrieved mean of the equivalent window using the TCCON spectroscopic database, which is taken as the reference in the present study due to its pedigree in validations for satellite missions.
- A posteriori error
  - Total uncertainty in the retrieved abundances of the methane isotopologues, including systematic and random errors. Wunch et al. (2010) states that systematic errors typically dominate for TCCON retrievals.
- δ^{13}C: Methane isotopologues abundances are typically expressed in the form of the following metric.

$$\delta^{13}C = \left(\frac{(^{13}CH_4/^{12}CH_4)_{sample}}{(^{13}CH_4/^{12}CH_4)_{VPDB}} - 1 \right) \times 1000‰, \quad (2)$$

where VPDB refers to Vienna Pee Dee Belemnite, an international reference standard for 13C assessment. Tropospheric methane typically exhibits a δ^{13}C value of roughly -47‰ (Rigby et al., 2017), and total column measurements from TCCON are unlikely to deviate from this value to a significant degree. Therefore this tropospheric δ^{13}C value acts as a useful proxy, to determine the stability and variability associated with retrievals of methane isotopologues from different spectral windows, spectroscopic databases, location and time using the tropospheric δ^{13}C value as a baseline.

In an ideal scenario we would compare our results with some reference results, however we are currently unaware of total column $^{13}CH_4$ retrieval data. We therefore perform our comparisons with respect to the TCCON spectroscopic database, under the assumption that biases are already present, which can be assessed at a later date if there is benefit to doing so.

2.3 Analysis criteria

There are two aspects to this study, the primary aspect is an assessment of the biases between spectral windows and spectroscopic databases w.r.t the two main methane isotpologues. TCCON typically aims for precision of <0.3% on methane retrievals, and has a rough estimate of 1% systematic uncertainties (dominated by in-situ calibration which vary depending on site (Wunch et al., 2015)). Therefore it is possible to judge the variations of the $^{12}CH_4$ between windows and databases based on these biases and precisions. In order to judge inter-window/spectroscopic database biases, we often compare the relative difference of the retrievals with respect to window 4 of the TCCON spectral database, henceforth described as the 'reference value'. We choose this window because it is the most commonly used in space based retrievals at this time (e.g. GOSAT), and the TCCON spectral database as it is the most established with TCCON retrievals. The relative difference is calculated as the difference between the retrieval and the reference value, divided by the reference value. This assessment is shown in Fig. 3.

In terms of $^{13}CH_4$, there are no published precision and accuracy requirements or statistics with TCCON. Fundamentally the final aim of retrieving $^{13}CH_4$ is to calculate δ^{13}C. δ^{13}C has been used to differentiate between methane source types (Fisher et al., 2017; Nisbet et al., 2016; Rigby et al., 2017; Rella et al., 2015), and variations of this value has been linked with variations in the global methane budget (Rigby et al., 2017; Mcnorton et al., 2016). How much δ^{13}C varies in the total varies in the total column is a complex issue (Weidmann et al., 2017; Malina et al., 2018, 2019), in-situ studies (Nisbet et al., 2016; Rigby et al., 2017; Fisher et al., 2017) all show that an uncertainty of «1‰ in δ^{13}C is required in order to determine natural annual variability at the surface. However, variability in δ^{13}C can be higher in the troposphere and stratosphere due to variability of the OH sink and the fractionation caused by OH (Röckmann et al., 2011; Buzan et al., 2016), with evidence that δ^{13}C can vary by up to 10‰ in different air parcels (Röckmann et al., 2011). Based on these factor, we assume a rough total column δ^{13}C variability of 1‰, which equates to a total uncertainty of <0.02 ppb on $^{13}CH_4$ retrievals, or roughly 0.1% of the total column. This is clearly an unrealistic target for individual retrievals, given the uncertainty requirements for $^{12}CH_4$ described above. Nevertheless precision errors will be low due to the nature of TCCON, and through the fact that TCCON sites are situated in a fixed position, allowing for long term averaging to reach a required precision target. Therefore one of the minor aims of this study is to identify how far away TCCON uncertainty (including systematic errors) is from the desired uncertainty of <1‰ δ^{13}C.

2.4 Sensitivity analysis

In addition to understanding any biases that may exist between spectroscopic databases and windows under nominal conditions, it is important to assess if these biases vary with respect to errors or assumptions in retrieval conditions, this type of assessment is known as a sensitivity analysis (Wunch et al., 2011; Hu et al., 2016). In this study we assess the impact of two key error sources, firstly how changing retrieval conditions over a series of TCCON measurements can affect biases, and secondly if uncertainty on the input retrieval information can impact bias magnitudes.

2.4.1 Local condition variations

Variations in the retrieval conditions throughout the course of a day of measurements are included in TCCON error budgets, for example artefacts can appear in TCCON retrievals at extreme SZA values (Wunch et al., 2011). We therefore investigate if the methane retrieval biases vary with respect to SZA and water vapour (retrieved by TCCON) changes through the course of a day at both TCCON sites. These dependencies are quantified by identifying the possible existence of a linear correlation (coefficient of determination) between the variations of water vapour and SZA against the bias of the retrieved methane isotopologue DMFs for each window and spectroscopic database, against the DMFs from window 4 from the TCCON spectroscopic database (otherwise known as the 'reference value').

2.4.2 A Priori and parameter errors

An important aspect of all trace gas retrievals are the sensitivities to uncertainties in the input a priori and parameter profile information. A priori information refers to quantities which are estimated as a part of the retrieval process (such as trace gases), and parameters refers to quantities necessary for retrieval, but are not estimated as a part of the retrieval process (such as temperature) (Rodgers, 2000). Here we investigate how the retrieved isotopologue DMFs vary between spectroscopic databases and windows when errors are applied to the a priori and parameter information. These profiles are derived from different models which carry inherent uncertainty e.g. (Wunch et al., 2011; Rahpoe et al., 2013), this can be assessed by perturbing the input parameter profiles and comparing the output results.

The a priori and parameter atmospheric data for the GFIT algorithm is based on two sources; the pressure, temperature and humidity data are drawn from the National Centers for Environmental Prediction (NCEP)/National Center for Atmospheric Research models (NCAR). The trace gas profiles are built from empirical models developed from a combination of data from atmospheric balloon borne sensors, and from the satellite instrument ACE-FTS (Wunch et al., 2010, 2011). We investigate the sensitivities of the retrievals to the following input parameter uncertainties.

Table 3. A priori and parameter error magnitude.

Error Source	Magnitude
Methane profile shift	2%
Methane profile shape	Swap seasonal profiles
Water vapour profile shift	10%
Pressure profile shift	2%
Temperature profile shift	2 K

The magnitudes identified in Table 3 mirror those used in a similar study focused on S5P/TROPOMI (Hu et al., 2016), given that S5P/TROPOMI validation is one of the focus points of this study. Since methane is the gas under investigation in this study, it is important to understand how shifting the input atmospheric profile affects the output. Since GFIT is a scalar retrieval algorithm, retrievals using an incorrect methane profile (e.g. tropopause in the incorrect layer) could induce biases which vary between windows and spectroscopic databases. Therefore the April and July Tsukuba methane profiles are swapped, and the August and October Ascension Island profiles are swapped to induce errors. Water vapour is the main interfering trace gas in these windows, and uncertainties in the starting knowledge of water vapour may yield different results from different windows or spectroscopic databases. GFIT directly retrieves methane and water vapour, but pressure and temperature are not included in the state vector and are not retrieved, meaning dependencies on pressure and temperature will not be removed in the retrieval process. Pressure column uncertainties can affect methane retrievals in two ways. The first is through the retrieval of O_2 which is used to convert the total column concentration of methane into DMFs, the second is through pressure dependence of spectroscopic absorption. For temperature, errors are introduced through the spectroscopic cross sections, Eq (3) describes the temperature dependency of the line intensity (An et al., 2011).

$$\frac{S(T)}{S(T_0)} = \frac{Q(T_0)}{Q(T)} exp(-\frac{hcE_0}{k}(\frac{1}{T} - \frac{1}{T_0})), \tag{3}$$

where $S(T)$ is the line intensity at temperature T, $Q(T)$ is the total partition function of the absorbing molecule at temperature T, $S(T_0)$ and $Q(T_0)$ are as before but at temperature T_0, E_0 is the lower state energy, and h, c and k are constants. Equation (3) suggests that if there are significant differences between the spectroscopic databases, most notably in the lower state energy level, then the temperature and pressure dependency uncertainty of the retrievals will vary depending on the database. Thus implying that the bias between spectroscopic databases can vary depending on spatial and temporal conditions.

To quantify the impact of these introduced errors we use two methods. Firstly the metrics described in sect 2.2 for 'retrieved values' are used for retrievals from April 2016 from the Tsukuba site, allowing for a direct comparison between the 'nominal cases' and the 'perturbed' sensitivity analysis cases. Secondly we use linear regression to compare the retrieved DMFs of $^{12}CH_4$ and $^{13}CH_4$ from cases where parameters errors have been introduced, and the original unperturbed cases. This linear regression is represented in two types of figure, the first qualitatively shows the correlation between perturbed and unperturbed cases for all windows, spectroscopic databases and TCCON sites. The second figure type shows the linear regression and

correlation statistics (slope, intercept, coefficient of determination and standard deviation) for the correlation plots in the first figure. These statistics are shown for all windows, spectroscopic databases and TCCON sites. All these results and figures are shown in Appendix C, and a summary, highlighting the impact of retrieval parameter uncertainty is shown in sect 3.5.

3 Results

3.1 Averaging kernels

Figure 1 shows example column averaging kernels for retrievals of $^{12}CH_4$ and $^{13}CH_4$ using windows 1, and 4-6 from selected observations at both Tsukuba and Ascension Island.

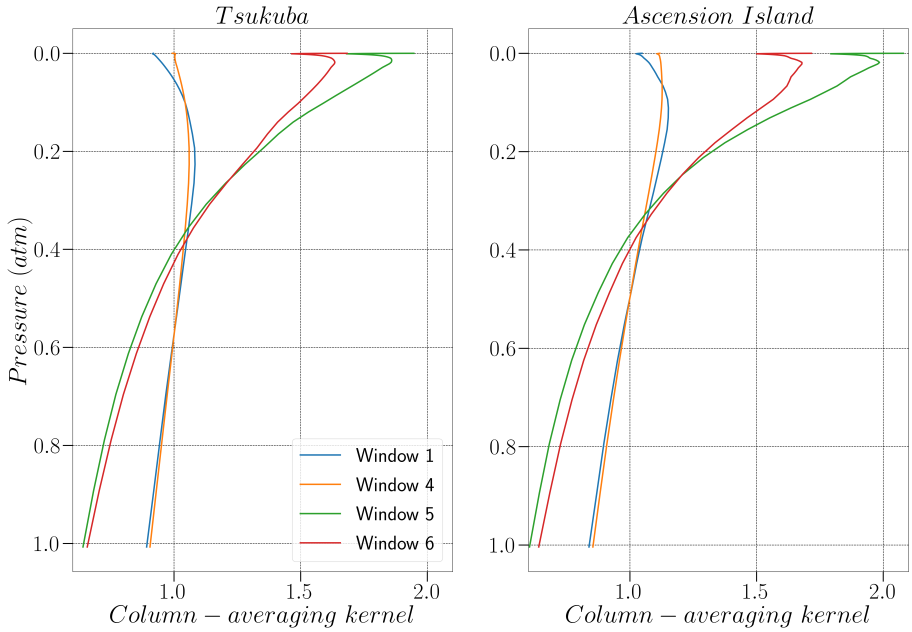

Figure 1. Column averaging kernels for typical retrievals of $^{12}CH_4$ and $^{13}CH_4$ from the Tsukuba TCCON site (left) and Ascension Island TCCON site (right) using the internal TCCON spectral database. The legend indicates the spectral window, for which the averaging kernels were calculated.

The $^{12}CH_4$ averaging kernels for both windows and both sites show little variation, and are similar to the CH_4 averaging kernels shown in (Wunch et al., 2011). The $^{13}CH_4$ averaging kernels show larger variation in the upper atmosphere, especially in the Ascension Island case, however this is not significant given the low concentration of $^{13}CH_4$ in the upper stratosphere. The shape of $^{13}CH_4$ averaging kernels is very similar to the shape of averaging kernels of CO from TCCON (Wunch et al., 2011), for all cases analysed in the present study. The similarity of the averaging kernels for the different windows shown in Fig 1 shows that the total columns retrieved from different fit windows can be compared directly, and that biases between windows can be attributed to other sources.

3.2 Transmission fit accuracy

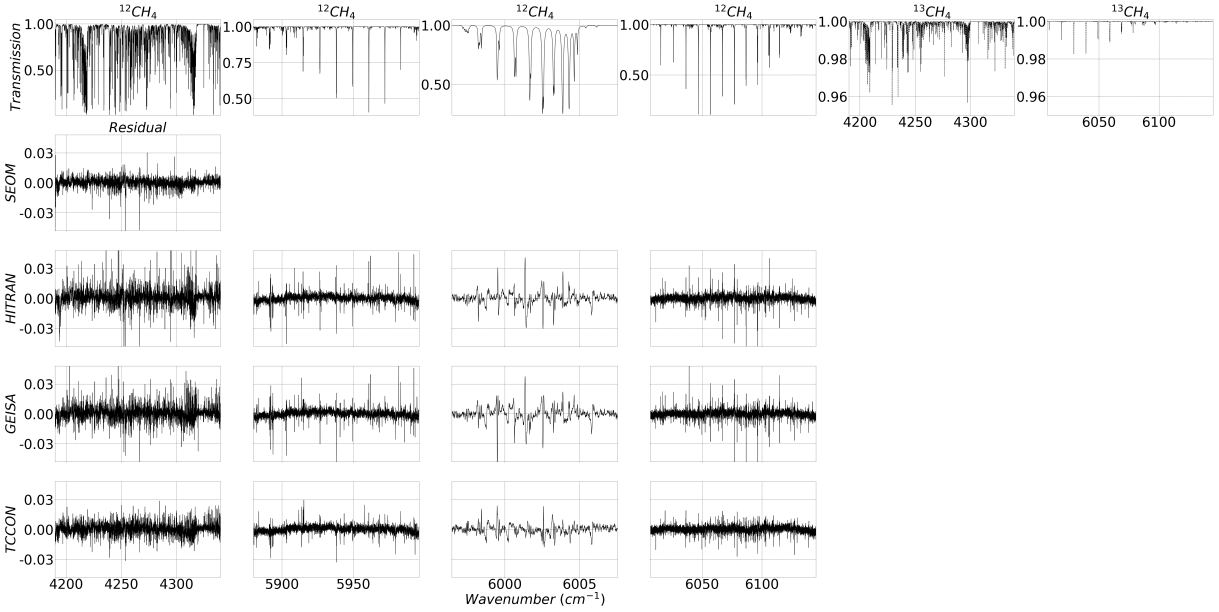

Figure 2. Example transmission spectra calculated from retrievals of $^{12}CH_4$ and $^{13}CH_4$ from the Tsukuba site in April 2016. Row 1 represents the calculated transmission of the target species ($^{12}CH_4$ for first four columns, $^{13}CH_4$ for the last two columns) using the TCCON spectroscopy database. The first four columns represent windows 1-4 respectively, the last two represent the windows of $^{13}CH_4$. The second row shows the residual transmission between the measured and calculated transmission from the SEOM-IAS database in window 1. Row 3 shows the residual transmission when the HITRAN2016 database is used, row 4 is the GEISA database and row 5 is the TCCON database.

Figure 2 shows the relative strengths of the absorption of the target trace gases in the selected spectral windows. We see that window 1 is a complex region with a large number of absorption lines including strong lines that saturate in the centre, and pronounced spectral overlap of lines. Windows 2-4 all show high levels of absorption but less line mixing/overlapping lines. The absorption by $^{13}CH_4$ in windows 5 and 6 are weak; window 1 contains significantly larger number of spectral lines compared to window 4. Both HITRAN2016 and GEISA2015 show significant residual transmission peaks in all of the windows. Quantitatively, the transmission statistics listed in Table 4 indicate that the SEOM-IAS retrieval has the best fit in window 1, with the TCCON database showing similar values. Note that the fit characteristics of window 1 are several times worse than any of the other windows explored in this study. We must take into account here that window 1 is wide, and that better fits could be obtained by splitting the window. Note that the column densities for all trace gases are fitted simultaneously, therefore changing the target gas for retrieval purposes (e.g. $^{12}CH_4$ or $^{13}CH_4$) does not change the fit residuals, hence this is why only the transmission values for $^{13}CH_4$ are shown, and no residuals.

For comparison purposes, Table A1 shows the same fit parameters, as shown in Table 4, but for an example of Ascension Island retrieval in October of 2016. The quality of fit is several times worse for the example of Ascension Island spectra, this is explained in Appendix A.

The key point is the relative fit values between the windows and spectral databases, which are similar to those shown in Table 4. This implies that the differences observed between the windows and databases exist, irrespective of time and location. Suggesting site and season are not major contributors to biases in window and spectroscopic database. The example transmission spectra shown in Fig 2 were captured with a solar zenith angle of 43°, with a similar air mass to other spectra captured on the same day, and the Ascension Island spectra were captured with a solar zenith angle of 22°, with a similar air mass to the Tsukuba spectra.

This analysis also shows that the GEISA database does not include any $^{13}CH_4$ lines in window 5, meaning that there will be no further analysis on this window w.r.t GEISA.

Table 4. Retrieval fit statistics for the case identified in Fig 1. The RMSE for each spectroscopic database is shown in row 1, with the results for windows 1-4 indicated in columns 1-4. The χ^2 values are shown in row 2 for each window.

	Window 1	Window 2	Window 3	Window 4
RMSE	TCCON: 4.438x10^{-3} HITRAN: 6.803x10^{-3} GEISA: 5.678x10^{-3} SEOM: 4.268x10^{-3}	TCCON: 3.076x10^{-3} HITRAN: 3.747x10^{-3} GEISA: 3.910x10^{-3} SEOM: nan	TCCON: 3.846x10^{-3} HITRAN: 5.392x10^{-3} GEISA: 6.01x10^{-3} SEOM: nan	TCCON: 2.680x10^{-3} HITRAN: 3.578x10^{-3} GEISA: 3.722x10^{-3} SEOM: nan
χ^2	TCCON: 0.392 HITRAN: 0.922 GEISA: 0.642 SEOM: 0.363	TCCON: 0.146 HITRAN: 0.216 GEISA: 0.235 SEOM: nan	TCCON: 0.0218 HITRAN: 0.0414 GEISA: 0.0532 SEOM: nan	TCCON: 0.132 HITRAN: 0.235 GEISA: 0.254 SEOM: nan

Note that the RMSE and χ^2 values for the $^{13}CH_4$ retrievals are identical to those indicated for $^{12}CH_4$ in the same window, and are therefore not repeated in Table 4.

3.3 Retrieval accuracy

Figure 3 shows a time series of 40 DMFs of $^{12}CH_4$ from measurements made on the 1st of April 2016 at the Tsukuba TCCON site. The top panel shows the time series over the course of the day for each spectral window and database in consideration. We see here that the maximum bias in retrieved $^{12}CH_4$ DMFs is roughly 50 ppb, between the HITRAN and GEISA 6002 cm^{-1} windows. The statistics in Table 5 suggest that window 3 has the largest deviation in DMFs w.r.t. spectroscopic databases, while window 1 has the lowest deviation. In general Table 5 suggests that there are significant variations in the retrieved DMFs in both spectral windows and spectral databases. The middle panel in Fig. 3 reveals a clear and constant bias between the reference values and the other windows, of up to 2%.

Table 5 suggests that window 1 shows the least variation, and window 3 has the most (largely driven by the GEISA retrievals). However, the inter-window variation suggests the least variation from the GEISA retrievals; the HITRAN retrievals show the

most. The bias values from the equivalent TCCON windows in general show the largest biases from the GEISA retrievals. However window 1 from the SEOM-IAS database shows the largest bias in this regard.

Retrieval uncertainties shown in the bottom panel of Fig 3 suggest a typical range of between 5 and 10 ppb, with the GEISA and HITRAN retrievals showing the highest errors. These errors are significantly lower than the persistent differences noted between the windows, meaning that these biases cannot be attributed to random retrieval uncertainties, and are likely due to differences in the spectroscopic databases.

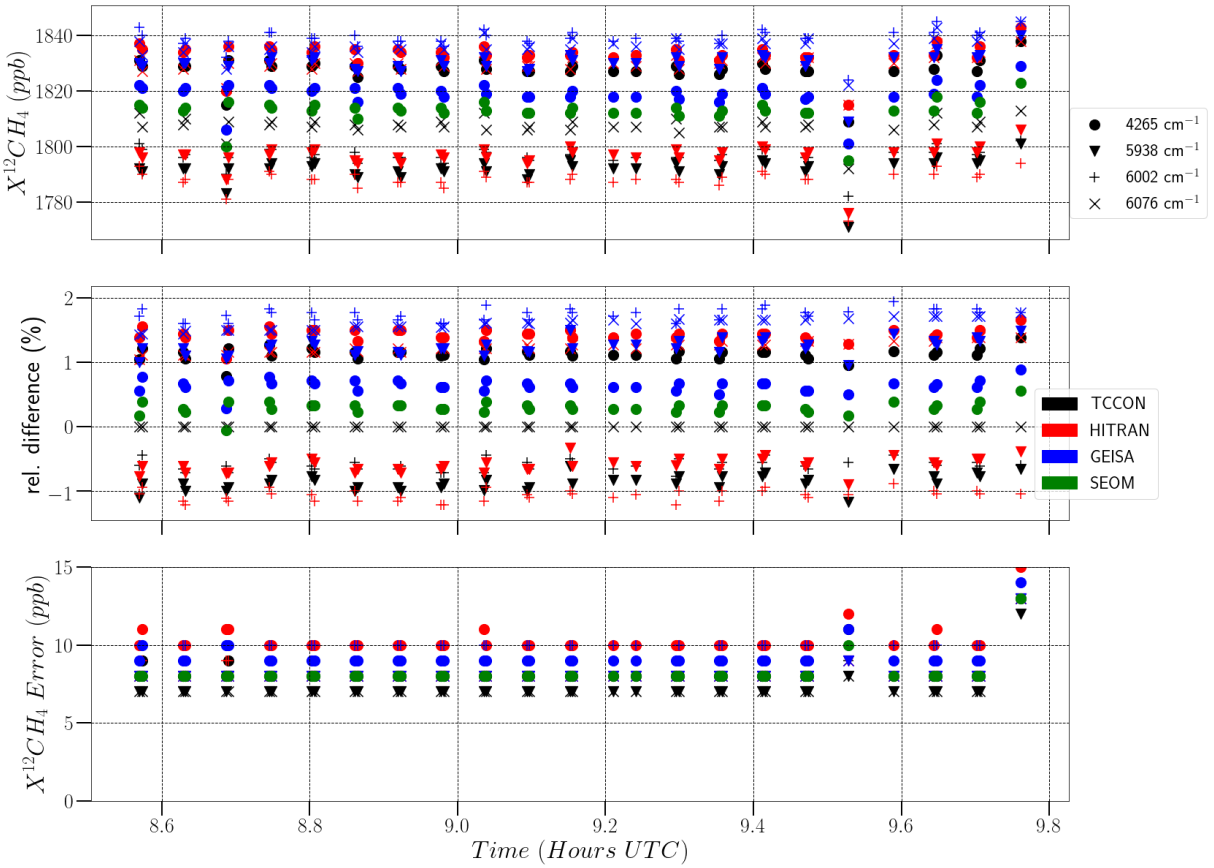

Figure 3. Retrieval time series for $^{12}CH_4$ DMFs from the Tsukuba site on 01/04/2016. The top panel indicates the retrieved DMFs of $^{12}CH_4$ in ppb for differing spectral windows and spectroscopic databases. The spectral windows are differentiated by line style, as shown in the legend in the top right corner. The databases are differentiated by colour, as indicated in the right of the middle panel. The middle panel shows the relative difference of the retrievals with respect to retrievals from window 4 of the TCCON database in ppb, illustrating the persistent behaviour of the spectroscopic-dependent and fit-window dependent differences. The bottom panel shows the total retrieval uncertainties in ppb.

Table 5. Statistics on 40 retrievals from the Tsukuba site on 01/04/2016 based on metrics identified in retrieval abundances subsection of section 2.2. The first row indicates the standard deviation of the retrieved DMFs from each window under study in this paper, with the target indicated for each window. The second data row indicates the standard deviation of the retrieved abundances of $^{12}CH_4$ for all windows present in each spectroscopic database, the third data row is as the second row, but for $^{13}CH_4$. The fourth to ninth data rows indicate the retrieved mean of the DMF for each window against the retrieved mean of the equivalent window using the TCCON spectroscopic database, with the window in question highlighted in the rows, and the spectroscopic database indicated in the columns.

Window	1 ($^{12}CH_4$)	2 ($^{12}CH_4$)	3 ($^{12}CH_4$)	4 ($^{12}CH_4$)	5 ($^{13}CH_4$)	6 ($^{13}CH_4$)
σ_{window} (ppb)	8.98	17.5	22.5	12.6	0.589	1.64
Database			TCCON	HITRAN	GEISA	SEOM-IAS
$\sigma_{inter-window}$ $^{12}CH_4$ (ppb)			16.5	20.0	9.15	N/A
$\sigma_{inter-window}$ $^{13}CH_4$ (ppb)			1.09	0.389	N/A	N/A

Database	HITRAN	GEISA	SEOM-IAS
bias (ppb; window 1)	5.36	8.90	15.1
bias (ppb; window 2)	4.92	38.1	N/A
bias (ppb; window 3)	8.49	42.4	N/A
bias (ppb; window 4)	22.3	28.9	N/A
bias (ppb; window 5)	1.22	N/A	0.00655
bias (ppb; window 6)	0.394	3.57	N/A

Considering a different set of retrievals, in this case 79 from the Ascension Island site on 01/10/2016, the statistics of which are highlighted in Table 6. These are shown to be similar in magnitude to those indicated in Table 5 (exemplified by the σ_{window} values), but are also shown to vary i.e in some cases magnitude increases, while others decrease. The $\sigma_{inter-window}$ values show similar magnitudes in both Tables 5 and 6, with HITRAN showing the largest inter-window variation, and GEISA the lowest. In general the bias values are similar in Table 5 and Table 6, however there are some differences. For example. there is a significantly larger bias for window 2 in HITRAN, and lower for window 4 in HITRAN. Window 4 bias for GEISA is also significantly lower. These results indicate that we can expect variations in retrieved methane biases depending on TCCON site and time of year.

Table 6. Statistics on 79 retrievals from the Ascension Island site on 01/10/2016 based on metrics identified in retrieval abundances subsection of section 2.2. The first row indicates the standard deviation of the retrieved DMFs from each window under study in this paper, with the target indicated for each window. The second data row indicates the standard deviation of the retrieved abundances of $^{12}CH_4$ for all windows present in each spectroscopic database, the third data row is as the second row, but for $^{13}CH_4$. The fourth to ninth data rows indicate the retrieved mean of the DMF for each window against the retrieved mean of the equivalent window using the TCCON spectroscopic database, with the window in question highlighted in the rows, and the spectroscopic database indicated in the columns.

Window	1 ($^{12}CH_4$)	2 ($^{12}CH_4$)	3 ($^{12}CH_4$)	4 ($^{12}CH_4$)	5 ($^{13}CH_4$)	6 ($^{13}CH_4$)
σ_{window} (ppb)	10.6	16.6	21.2	14.8	0.981	2.79
Database			TCCON	HITRAN	GEISA	SEOM-IAS
$\sigma_{inter-window}$ $^{12}CH_4$ (ppb)			16.3	19.4	11.1	N/A
$\sigma_{inter-window}$ $^{13}CH_4$ (ppb)			1.83	2.30	N/A	N/A

Database	HITRAN	GEISA	SEOM-IAS
bias (ppb; window 1)	7.76	8.47	19.2
bias (ppb; window 2)	9.15	35.4	N/A
bias (ppb; window 3)	7.41	37.6	N/A
bias (ppb; window 4)	10.6	16.7	N/A
bias (ppb; window 5)	1.45	N/A	0.414
bias (ppb; window 6)	2.45	3.38	N/A

For further analysis on the biases presented in Fig 3 and Tables 5 and 6, we also show additional retrieval statistics for 40 retrievals from Tsukuba on 07/07/2016 (Table B1), and 243 retrievals from Ascension Island on 23/08/2016 (Table B2). Comparing the statistics from Fig. 3 and Tables 5, 6, B1 and B2, we note similar magnitudes in all of the presented statistics, and similar magnitudes in the differences when comparing the results from different windows or spectroscopic database. For example the σ_{window} value in window 1 is between 8.98 and 10.6 ppb depending on TCCON site and time of year of retrievals, but for window 3 it is between 21.2 and 23.7 ppb. In the cases shown in this study, σ_{window} is at a minimum in window 1, and at a maximum in window 3, with window 3 showing up to roughly x2.5 larger deviation than window 1. Windows 2 and 4 show more variation, and often show similar magnitudes. The implications of these results are that windows 1 and 3 are more consistent across the databases, and windows 2 and 4 are less so. $\sigma_{inter-window}$ results consistently show the GEISA2015 database has the lowest deviation in $^{12}CH_4$ DMFs across all bands, but also show the most variation across sites and season (4.25 ppb). HITRAN2016 shows the highest $\sigma_{inter-window}$ results, and the TCCON database is in between, but shows almost no variation in values across sites and seasons. Considering the biases of each spectral window from each spectroscopic database against the equivalent window from the TCCON spectroscopic database, there is evidence of some patterns emerging. For example, the HITRAN2016 database shows the lowest bias in each window w.r.t. the TCCON database, while the GEISA2015 database shows the highest and window 1 for all spectroscopic databases consistently shows largely

constant values across all TCCON sites and seasons. However, there is also significant evidence of changing behaviours, window 4 especially varies by as much as 300% between sites and seasons. The results from this analysis suggest that window 1 is the most consistent and is less sensitive to changing conditions, while other windows show much more variation with differing conditions.

For $^{13}CH_4$ DMFs we see similar results to $^{12}CH_4$ DMFs, window 5 typically shows the least variation, and the GEISA2015 database shows the largest differences.

3.4 Calculation of δ^{13}C values

Based on Eq 2, we can calculate the δ^{13}C values for both Tsukuba and Ascension Island TCCON sites for the days shown in this study, this allows to quickly determine how accurate any retrievals of $^{13}CH_4$ DMFs from TCCON are. Here we used the same spectral windows to calculate these values, i.e. windows 1 and 5, and windows 4 and 6. For the δ^{13}C values we calculate an averaged value for the whole day.

Table 7. Daily averaged values of δ^{13}C from both TCCON sites for two $^{12}CH_4$ and $^{13}CH_4$ window combinations for each spectral database.

δ^{13}C	TCCON windows 1 & 5	TCCON windows 4 & 6	HITRAN windows 1 & 5	HITRAN windows 4 & 6	GEISA windows 4 & 6	SEOM windows 1 & 5
Tsukuba 01/04/2016	-116‰	-1.52‰	-59.1‰	-33.1‰	-193‰	-109‰
Tsukuba 07/07/2016	-173‰	74.5‰	-159‰	296‰	-202‰	-143‰
Ascension Island 23/08/2016	-108‰	-92.4‰	-104‰	-8.47‰	-297‰	-95.0‰
Ascension Island 01/10/2016	-115‰	43.6‰	-46.7‰	160‰	-134‰	-84.2‰

Table 7 shows that the δ^{13}C values calculated from the windows 1 and 5 combination are partially consistent across sites and dates (with the exception of the July retrievals from Tsukuba), while the values calculated from windows 4 and 6 show much more variation. However, there is still significant variation across all cases that cannot be accounted for purely by precision errors. We therefore assert that in the case of TCCON retrievals, the dominant error in δ^{13}C retrievals are spectroscopic errors. It is also clear that there is still not possible to make useful retrievals of δ^{13}C at this time, with both improvements in spectroscopic parameters and retrieval accuracy necessary.

3.5 Sensitivity analysis

3.5.1 Local condition variations

Here we investigate if locally changing conditions impact biases between spectroscopic databases and windows, as described in sect 2.4.1. Firstly sensitivity to variations in water vapour concentrations are considered in Table 8 below.

Table 8. Linear relationship expressed at the coefficient of determination (R^2) between daily variations of water vapour for each TCCON site and day considered in this study, and the bias of $^{12}CH_4$ DMFs against the 'reference value'.

Database/Window	Tsukuba April 2016	Tsukuba July 2016	Ascension August 2016	Ascension October 2016
TCCON Window 1	0.03	0.2	0.0	0.07
TCCON Window 2	0.3	0.2	0.2	0.6
TCCON Window 3	0.03	0.01	0.002	0.1
HITRAN Window 1	0.01	0.3	0.009	0.003
HITRAN Window 2	0.3	0.2	0.1	0.5
HITRAN Window 3	0.1	0.01	0.03	0.5
HITRAN Window 4	0.6	0.09	0.2	0.7
GEISA Window 1	0.01	0.3	0.002	0.03
GEISA Window 2	0.3	0.2	0.2	0.7
GEISA Window 3	0.2	0.04	0.07	0.6
GEISA Window 4	0.5	0.1	0.2	0.7
SEOM Window 1	0.03	0.002	0.05	0.2

The coefficients of determination shown in Table 8 generally indicate that there is limited or no relationship between the variability of water vapour content in the atmosphere and the bias between retrieved DMFs of $^{12}CH_4$ from differing windows and spectroscopic databases. Yet, some of the results shown for the Ascension Island October 2016 case suggests otherwise, with TCCON window 2, HITRAN window 4 and GEISA windows 2-4 all showing some indication of a linear relationship. In addition, window 4 for all spectroscopic databases shows stronger linear relationships than any other of the windows presented in Table 8, although this is not consistent for all of the cases indicated here. However, it is difficult to explain these relationships purely due to water variability. Table D1 outlines some of the conditions prevalent at each site on the days in question, with both Ascension Island cases showing roughly similar average water vapour content, and similar variability, meaning that the relationships shown in Table 8 are unlikely to be purely down in water vapour. To investigate further, we identify the linear relationship between SZA and retrievals biases in Table 9 below.

Table 9. Linear relationship expressed at the coefficient of determination (R^2) between daily variations of SZA for each TCCON site and day considered in this study, and the bias of $^{12}CH_4$ DMFs against the 'reference value'.

Database/Window	Tsukuba April 2016	Tsukuba July 2016	Ascension August 2016	Ascension October 2016
TCCON Window 1	0.01	0.2	0.05	0.09
TCCON Window 2	0.2	0.3	0.3	0.7
TCCON Window 3	0.03	0.0	0.0	0.08
HITRAN Window 1	0.0	0.2	0.1	0.0
HITRAN Window 2	0.2	0.2	0.2	0.6
HITRAN Window 3	0.1	0.0	0.1	0.5
HITRAN Window 4	0.9	0.8	0.9	0.8
GEISA Window 1	0.0	0.2	0.1	0.03
GEISA Window 2	0.3	0.3	0.5	0.8
GEISA Window 3	0.2	0.02	0.5	0.7
GEISA Window 4	0.9	0.9	0.9	0.8
SEOM Window 1	0.07	0.02	0.01	0.1

The results shown in Table 9 closely align with those shown in Table 8, in that the Ascension Island October 2016 case shows a number of cases with strong linear correlation, while the majority of the Tsukuba retrievals largely indicate no relationship (except in window 4). As with Table 8, the results from window 1 show the weakest relationships, but the results from window 4 from all spectroscopic databases show strong indication of bias sensitivity to SZA. Therefore these results suggest that biases between spectroscopic databases and windows can vary with changing SZA in specific windows. It is likely not a coincidence that the strongest linear correlations in Tables 8 and 9 occur in the same cases. Table D1 indicates the range of SZAs where spectra were captured for each TCCON site, it clearly shows Ascension Island spectra are captured under a wider range of SZAs than Tsukuba, in addition the October retrievals from Ascension Island have a mean SZA of 50°, and the retrievals from Tsukuba and Ascension Island from other seasons have mean SZA of <50°. The implication is that variations in water vapour have more effect on biases between windows and spectroscopic databases when higher SZAs are involved.

3.5.2 A priori and parameter errors

The analysis for the a priori and parameter errors discussed in sect 2.4.2 is shown in Appendix C, split into results for each of the cases described in Table 3. A summery of these results is presented here.

The effect of adding a 2% profile shift to the a priori methane profiles is shown in Appendix C1. Comparing the results from Table 5 and Table C1, only minor differences are shown, implying that for the case of April 2016 in Tsukuba, adding a 2% bias to the methane profile has minimal impact. Figures C1 and C2 build on this by showing close linear relationships between the unperturbed perturbed retrieved DMFs for all windows, spectroscopic databases and TCCON sites considered in

this study, suggesting that biases in the a priori methane profile have minimal effect on window and spectroscopic database biases. When methane profile shapes were switched (Appendix C2), we can see through a comparison of Tables 5 and C2 that there is an impact. For example there is a 9.7% difference in the σ_{window} of window 2, and a 7.2% difference in the TCCON $\sigma_{inter-window}$ for $^{12}CH_4$. Figures C3 and C4 elaborate on this impact, showing variation in the responses for each window and database, as well as a lower impact in results from Ascension Island. Appendix C3 shows how uncertainty in the a priori knowledge of water vapour affects retrieval biases; comparisons between Tables 5 and C3 show minimal differences, with only windows 2 and 4 showing notable change. However, Table D1 does show the April 2016 Tsukuba case as having low water vapour concentration and minor variation. Figures C5 and C6 indicate the higher water vapour concentrations and variability in the other cases have more impact, especially in Tsukuba in July. Indicating that uncertainty in the water vapour column affects inter-window/spectroscopic database biases more significantly in high humidity atmospheres. Figures C5 and C6 also show that windows 2 and 4 are the most affected by uncertainty in the a priori water vapour column. The effects of pressure profile uncertainty are shown in Appendix C4; Table C4 indicates significant changes due to this perturbation, with σ_{window} for window 4 showing a 2.4% difference and a 7.5% difference when considering $\sigma_{inter-window}$ for HITRAN. Bias values range between databases and windows, with window 3 showing the most change (1.5% in the case of HITRAN). Building on these results, the linear correlation plots of Figs C7 and C8 show that each site and season have different sensitivities to perturbations in the pressure profile, with window 2 generally indicating the most sensitivity. Finally, the effects of a 2 K temperature perturbation are investigated in Appendix C5, where again differing bands and spectroscopic databases show different sensitivities. For example, the difference between Table 5 and C5 in the σ_{window} for window 4 is 4.5%, while there is no change in window 3. The $\sigma_{inter-window}$ values show variation, with the TCCON database showing a 6% difference between perturbed and non-perturbed cases. For the biases w.r.t. the TCCON database, window 2 shows the most sensitivity, with a 16% and 2.6% difference for HITRAN and GEISA. In summary the results from this analysis suggest the inter-window and inter-database biases identified in section 3.3 are variable depending on the uncertainty associated with the a priori and parameter information. Methane profile shape and pressure profile errors are especially significant, but in all cases the errors effect different bands in different databases differently, with windows 2 and 4 being particularly sensitive to errors. In addition the local conditions have an impact, with biases varying depending on the TCCON site and season.

An assessment of the sensitivity of $^{13}CH_4$ to errors in the a priori and parameter profiles is also included in Appendix C, generally indicating high sensitivity to all error sources. Windows 5 and 6 vary in their sensitivity, with the different spectroscopic databases showing similar sensitivity in window 5, but very different ones in window 6.

4 Discussion

We find significant variations in retrieved DMFs across all of the considered windows and spectroscopic databases in this study, are most likely due to imperfections in the spectroscopic parameters. The results identify that each database reacts differently to a priori and parameter uncertainty, as well as variability in local conditions. It is difficult to attribute the biases we have

identified to specific spectroscopic parameters errors, due to the range of parameters used, and it is beyond the scope of this paper to do so.

In addition to differences between the spectroscopic databases, we have shown that there are significant differences between the spectral windows used for retrieving methane isotopologues. This would not be not a significant problem if the systematic biases between the windows were constant. However, we have shown that retrieval results from each window responds differently to uncertainty in the a priori and parameter profiles. We conclude that there is likely to be an underlying bias in all TCCON data that varies from retrieval to retrieval, and day to day.

We note that advancements are currently being tested on retrievals of methane from TCCON spectra, for example with the "SFIT4" algorithm (Zhou et al., 2019), which allows for profile retrievals and would therefore not be subject to the methane profile errors investigated in this study. The next generation of GGG2014, the so called "GGG2020" has also recently been released. This update includes an improved spectroscopic database and the ability to use non-Voigt line shapes for methane. Therefore the updates to GGG and the use of other algorithms in this study could yield improved results. However, it is likely that the bias problems identified in this study may remain to some degree.

In addition to understanding the biases associated with retrieving $^{12}CH_4$ DMFs from TCCON spectra with differing spectroscopic databases, this study touches a question that is of some interest to the community, “can we calculate realistic and constant δ^{13}C values from TCCON”. The results from this study suggest not this is not yet possible, based on the results shown in Table 7 and given that the tropospheric average δ^{13}C value is assumed to be -47‰ (Sherwood et al., 2016), and our results are significantly different from this. We expect that large deviations from this value is unlikely, given that TCCON retrieves total column estimates, and not in-situ samples. This assumption of -47‰ is a little unfair, since this is an assumption based on lower tropospheric averages, and does not take into account sink processes that occur further up into the atmosphere. For example Rigby et al. (2017) assume a -2.6‰ fractionation due to the chlorine sink in the stratosphere, and significant fractionation does occur in the troposphere with the OH sink (Röckmann et al., 2011). However, it can be argued here that the priority in calculating an accurate value of δ^{13}C from TCCON is a full assessment of all of the systematic biases present in the retrievals, most notably the spectroscopic biases, before discussion of the true δ^{13}C value of the total column.

5 Conclusions

In this study, using the GGG2014 retrieval environment we retrieve $^{12}CH_4$ DMFs from two TCCON sites, with the aim of understanding the biases associated with retrieving methane isotopologues in the TROPOMI spectral region as opposed to standard TCCON methane windows. Four different windows covering the spectral range of the future S5/UVNS instrument and the current S5P/TROPOMI instrument are used. Three of the windows are routinely used in TCCON products, but the TROPOMI window in the 4190-4340 cm^{-1} range is not. We use four sources of spectroscopic parameters, the HITRAN2016, GEISA2015, SEOM-IAS and internal TCCON database in order to assess the impact of spectroscopic database uncertainties. Measurements are taken from two TCCON sites (Tsukuba, and Ascension island) to provide a range in atmospheric conditions.

We found that the SEOM-IAS and internal TCCON spectroscopy databases (with the SEOM-IAS database limited to window 1/4190-4340 cm^{-1} spectral range) showed the lowest biases and errors. The SEOM-IAS database shows the best fit metrics, the most consistent retrievals, and the lowest sensitivity to a priori and parameter errors.

We find significant levels of bias between the retrieved $^{12}CH_4$ DMFs both in terms of spectral window and spectroscopic database. In some cases, similar windows from different spectroscopic databases differ by as much as 50 ppb, which is much larger than the precision and accuracy requirements of TROPOMI. These biases remain consistent between TCCON sites, implying systematic errors in the spectroscopic parameters. Window 1 (4190-4340 cm^{-1}) shows the lowest variation between the databases, typically < 10 ppb, and the short window 3 (6002 cm^{-1}) shows the most variation, typically > 20 ppb.

The sensitivity of the retrieved $^{12}CH_4$ DMFs to locally changing conditions such as water vapour and to uncertainty in the a priori and parameter profiles is investigated. We find that Window 1 from the SEOM-IAS database is the most insensitive to these errors, while windows 2 and 4 are the most sensitive.

The analysis in this study led to two key conclusions, firstly we recommend including the TROPOMI SWIR spectral region (in this study, window 1) into future TCCON methane retrievals, due to the consistency of the retrievals presented in this study, and the consistency of the retrievals in the face of sensitivity errors. Secondly, based on major deviations between retrievals from different spectroscopic databases, and the differing sensitivities of spectroscopic databases and windows to sensitivity errors, we call for further investigation into how to incorporate these errors into future satellite and TCCON retrievals.

$^{13}CH_4$ DMFs are also retrieved in parallel to $^{12}CH_4$, but are found to be too in-accurate for the communities needs. It was argued that the static nature of TCCON sites could reduce the high precision errors over a long period, however fundamental accuracy issues in the spectroscopic databases must be overcome first.

Code and data availability. The GGG2014 retrieval environment is available at https://tccon-wiki.caltech.edu, and TCCON L1b spectra are available upon discussion with the relevent site PI

Appendix A: Transmission

Example transmission for Ascension Island.

Table A1. Retrieval fit statistics for example Ascension Island retrieval in October 2016. The RMSE for each spectroscopic database is shown in row 1, with the results for windows 1-4 indicated in columns 1-4. The χ^2 values are shown in row 2 for each window.

	Window 1	Window 2	Window 3	Window 4
RMSE	TCCON: 8.748x10^{-3} HITRAN: 1.061x10^{-2} GEISA: 9.880x10^{-3} SEOM: 8.508x10^{-3}	TCCON: 6.488x10^{-3} HITRAN: 7.035x10^{-3} GEISA: 7.296x10^{-3} SEOM: nan	TCCON: 6.482x10^{-3} HITRAN: 8.738x10^{-3} GEISA: 8.887x10^{-3} SEOM: nan	TCCON: 6.253x10^{-3} HITRAN: 6.723x10^{-3} GEISA: 6.906x10^{-3} SEOM: nan
χ^2	TCCON: 1.524 HITRAN: 2.241 GEISA: 1.944 SEOM: 1.441	TCCON: 0.648 HITRAN: 0.762 GEISA: 0.820 SEOM: nan	TCCON: 0.0670 HITRAN: 0.112 GEISA: 0.116 SEOM: nan	TCCON: 0.716 HITRAN: 0.828 GEISA: 0.874 SEOM: nan

Concerning the differences in fit quality between the Tsukuba and the Ascension Island TCCON instruments: both instruments run according to TCCON specifications but their respective configurations are not exactly the same. This is normal and necessary as different sites need local adjustments to account for different local conditions such as altitude, humidity or cloud conditions. Most of the effects caused by such individual configurations are removed by the differential CO_2 and CH_4 DMF retrievals but will affect individual spectra.

In the case of Tsukuba and Ascension, the configuration effects cannot be compared directly except for detector noise, which turned out to be comparable. However, the signal on the detector of the Ascension Island instrument is at least 50% lower than that of the Tsukuba instrument.

Likely reasons are:

1) The Ascension FTS runs on a higher spectral resolution (0.014 cm^{-1} vs. 0.02 cm^{-1}) and a faster scanner speed (10 kHz vs. 7.5 kHz). Both reduce integration time per spectral pixel.

2) The illumination of the InGaAS detector on Ascension is kept low on purpose to avoid saturation. This setting cannot be readjusted in between site visits and has to last for months.

3) The solar tracker has known issues with pointing at the centre of the sun at low SZAs but cannot be replaced easily. In addition, dust buildup on the solar tracker mirrors reduces the reflectivity of the mirrors quickly. They are cleaned weekly but a signal loss in the order of 20% over a few days is not uncommon.

Appendix B: Retrieval statistics

Table B1. Statistics for 40 retrievals from Tsukuba on 07/07/2016 based on metrics identified in retrieval abundances subsection of section 2.2. The first row indicates the standard deviation of the retrieved DMFs from each window under study in this paper (σ_{window}), with the target indicated for each window. The second data row indicates the standard deviation of the retrieved abundances of $^{12}CH_4$ for all windows present in each spectroscopic database ($\sigma_{inter-window}$), the third data row is as the second row, but for $^{13}CH_4$. The fourth to ninth data rows indicate the retrieved mean of the DMF for each window against the retrieved mean of the equivalent window using the TCCON spectroscopic database (bias), with the window in question indicated in the rows, and the spectroscopic database indicated in the columns.

Window	1 ($^{12}CH_4$)	2 ($^{12}CH_4$)	3 ($^{12}CH_4$)	4 ($^{12}CH_4$)	5 ($^{13}CH_4$)	6 ($^{13}CH_4$)
σ_{window} (ppb)	9.42	15.7	23.7	18.5	0.26	4.14
Database			TCCON	HITRAN	GEISA	SEOM-IAS
$\sigma_{inter-window}$ $^{12}CH_4$ (ppb)			16.4	18.1	10.5	N/A
$\sigma_{inter-window}$ $^{13}CH_4$ (ppb)			2.40	4.63	N/A	N/A

Database	HITRAN	GEISA	SEOM-IAS
bias (ppb; window 1)	6.54	9.74	17.2
bias (ppb; window 2)	8.87	36.4	N/A
bias (ppb; window 3)	1.23	49.4	N/A
bias (ppb; window 4)	34.6	41.9	N/A
bias (ppb; window 5)	0.338	N/A	0.307
bias (ppb; window 6)	4.88	5.10	N/A

Table B2. Statistics for 243 retrievals from Ascension Island on 23/08/2016 based on metrics identified in retrieval abundances subsection of section 2.2. The first row indicates the standard deviation of the retrieved DMFs from each window under study in this paper (σ_{window}), with the target indicated for each window. The second data row indicates the standard deviation of the retrieved abundances of $^{12}CH_4$ for all windows present in each spectroscopic database ($\sigma_{inter-window}$), the third data row is as the second row, but for $^{13}CH_4$. The fourth to ninth data rows indicate the retrieved mean of the DMF for each window against the retrieved mean of the equivalent window using the TCCON spectroscopic database (bias), with the window in question highlighted in the rows, and the spectroscopic database indicated in the columns.

Window	1 ($^{12}CH_4$)	2 ($^{12}CH_4$)	3 ($^{12}CH_4$)	4 ($^{12}CH_4$)	5 ($^{13}CH_4$)	6 ($^{13}CH_4$)
σ_{window} (ppb)	10.0	18.3	23.2	17.9	1.02	3.22
Database			TCCON	HITRAN	GEISA	SEOM-IAS
$\sigma_{inter-window}$ $^{12}CH_4$ (ppb)			16.4	18.1	13.4	N/A
$\sigma_{inter-window}$ $^{13}CH_4$ (ppb)			1.69	1.99	N/A	N/A

Database	HITRAN	GEISA	SEOM-IAS
bias (ppb; window 1)	6.30	8.99	17.0
bias (ppb; window 2)	7.16	37.5	N/A
bias (ppb; window 3)	5.71	42.8	N/A
bias (ppb; window 4)	21.0	27.4	N/A
bias (ppb; window 5)	0.368	N/A	0.307
bias (ppb; window 6)	1.90	3.87	N/A

Appendix C: Sensitivity errors

C1 Methane Profile shift

An analysis on the impact of inserting a 2% methane profile shift error into the a priori information is included in this sub-appendix. Table C1 below allows for direct comparison with Table 5 of the impact of this shift.

Table C1. Statistics as Table 5 for the methane profile shift case identified in sect. 2.4. Data is for April 2016 Tsukuba retrievals.

Window	1 ($^{12}CH_4$)	2 ($^{12}CH_4$)	3 ($^{12}CH_4$)	4 ($^{12}CH_4$)	5 ($^{13}CH_4$)	6 ($^{13}CH_4$)
σ_{window} (ppb)	9.03	17.6	22.5	12.9	0.591	1.65
Database			TCCON	HITRAN	GEISA	SEOM-IAS
$\sigma_{inter-window}$ $^{12}CH_4$ (ppb)			16.5	19.9	9.32	N/A
$\sigma_{inter-window}$ $^{13}CH_4$ (ppb)			1.09	0.388	N/A	N/A

Database	HITRAN	GEISA	SEOM-IAS
bias (ppb; window 1)	5.36	9.26	15.1
bias (ppb; window 2)	5.15	38.4	N/A
bias (ppb; window 3)	8.21	42.5	N/A
bias (ppb; window 4)	22.4	28.9	N/A
bias (ppb; window 5)	1.22	N/A	0.00313
bias (ppb; window 6)	0.395	3.58	N/A

Further analysis is below, showing the linear relationship between the original standard retrievals, and the perturbed retrievals. All Tsukuba and Ascension island retrievals considered in this study are included in these figures.

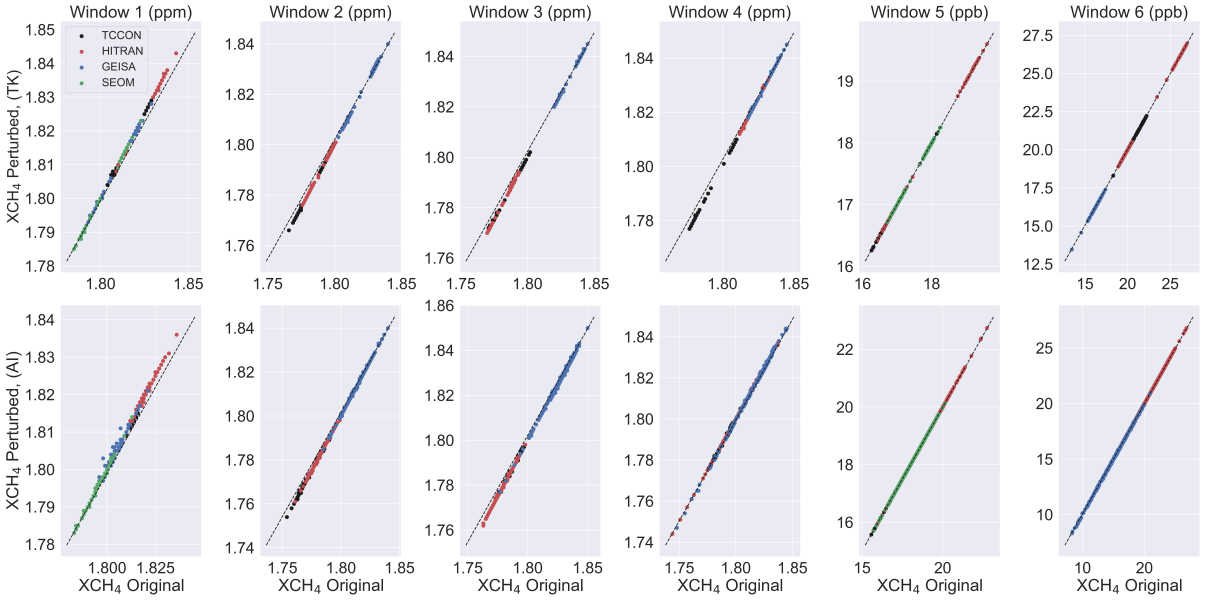

Figure C1. Series of scatter plots showing unperturbed retrieved DMFs $^{12}CH_4$ and $^{13}CH_4$ from the cases indicated in sect. 3.3 and Appendix B, against these cases when perturbed by a 2% shift to the a priori methane profile. Each column indicates the window under consideration, the top row is for Tsukuba data (TK), and the bottom row is for Ascension Island data (AI). The colours in the plots are consistent with the rest of this paper in indicating the spectroscopic database. The units for all axes are indicated in the titles.

Figure C1 qualitatively indicates some sensitivity to methane profile perturbation, the linear regression statistics of Fig. C1 are shown in Fig C2, including slope, intercept, coefficient of determination and standard deviation.

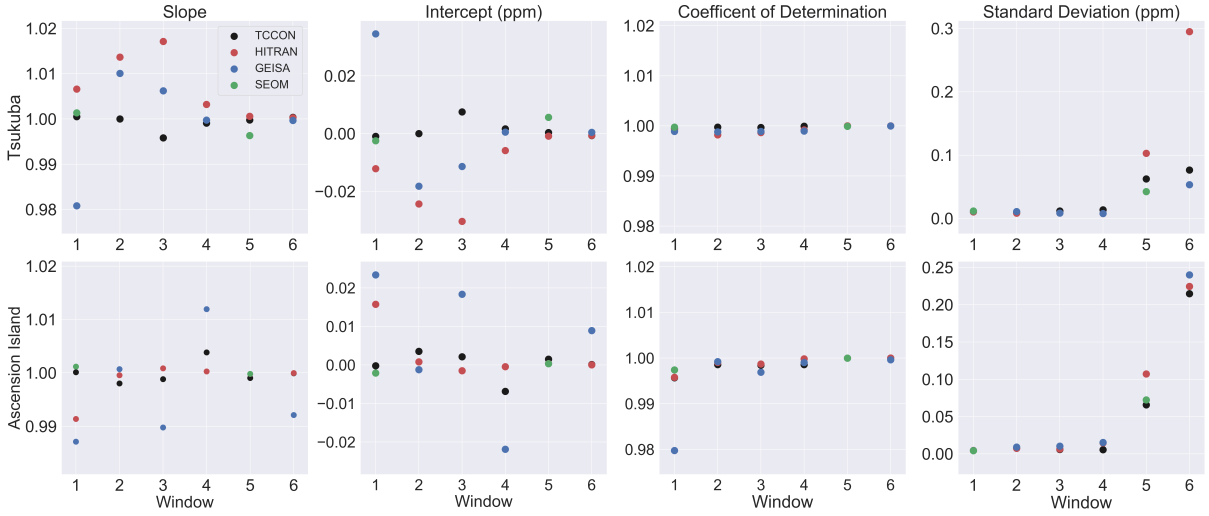

Figure C2. Plot indicating the linear statistical relationship between the perturbed and unperturbed $^{12}CH_4$ and $^{13}CH_4$ DMFs indicated in Fig C1. The x-axis for all plots indicates the retrieval window under consideration. The first column shows the values for the linear slope, the second column is the linear intercept, the third column is the coefficient of determination and the fourth column is the standard deviation. The first row indicates retrievals from Tsukuba and the second row shows retrievals from Ascension island. The colours in the plots are consistent with the rest of this paper in indicating the spectroscopic database.

Figure C2 builds on the quantification in Table C1, and shows low dependency on errors in a methane profile shift, with no clear patterns between windows and spectroscopic databases.

C2 Methane Profile Shape

An analysis on the impact of inserting a methane profile shape error into the a priori information is included in this sub-appendix. The retrievals from Tsukuba April 2016 use the methane profile of Tsukuba July 2016 and vice versa, and the retrievals from Ascension island August 2016 use the methane profile of Ascension island October 2016 and vice versa. Table C2 below allows for direct comparison with Table 5 of the impact of this shift.

Table C2. Statistics as Table 5 for the methane profile shape change case identified in sect. 2.4. Data is for April 2016 Tsukuba retrievals.

Window	1 ($^{12}CH_4$)	2 ($^{12}CH_4$)	3 ($^{12}CH_4$)	4 ($^{12}CH_4$)	5 ($^{13}CH_4$)	6 ($^{13}CH_4$)
σ_{window} (ppb)	8.98	19.12	23.6	13.02	0.569	1.63
Database			TCCON	HITRAN	GEISA	SEOM-IAS
$\sigma_{inter-window}$ $^{12}CH_4$ (ppb)			17.7	21.1	9.15	N/A
$\sigma_{inter-window}$ $^{13}CH_4$ (ppb)			1.11	0.409	N/A	N/A

Database	HITRAN	GEISA	SEOM-IAS
bias (ppb; window 1)	5.46	8.33	15.2
bias (ppb; window 2)	4.77	41.6	N/A
bias (ppb; window 3)	8.33	44.9	N/A
bias (ppb; window 4)	22.1	29.5	N/A
bias (ppb; window 5)	1.18	N/A	0.0256
bias (ppb; window 6)	0.39	3.53	N/A

530 Further analysis is below, showing the linear relationship between the original standard retrievals, and the perturbed retrievals. All Tsukuba and Ascension island retrievals considered in this study are included in these figures.

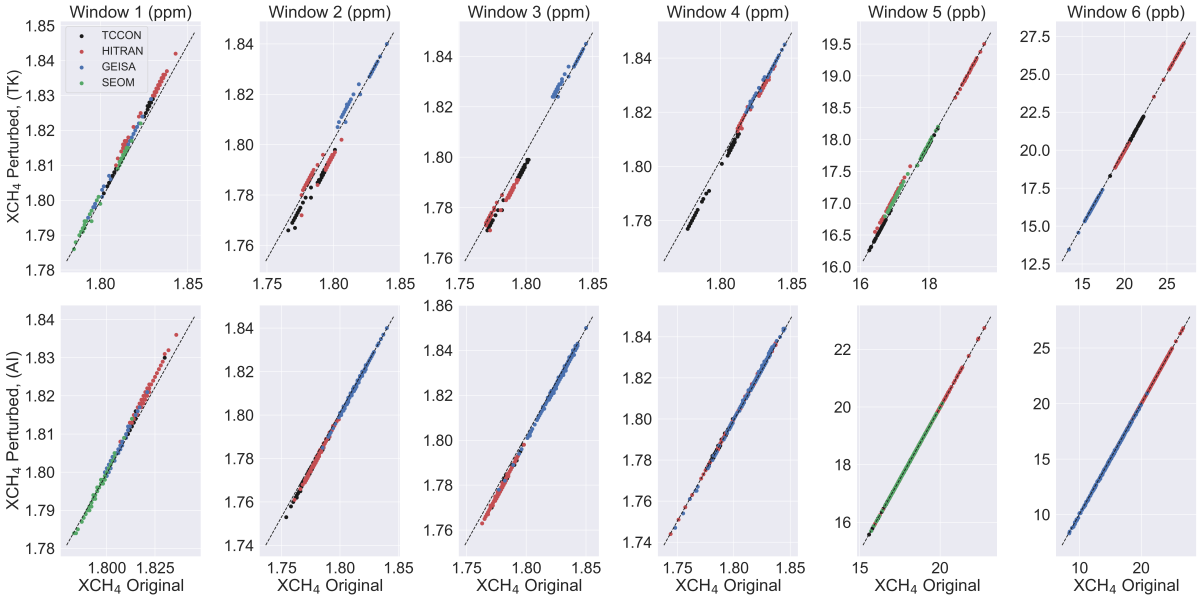

Figure C3. Series of scatter plots showing unperturbed retrieved DMFs $^{12}CH_4$ and $^{13}CH_4$ from the cases indicated in sect. 3.3 and Appendix B, against these cases when perturbed by a change to the a priori methane profile. Each column indicates the window under consideration, the top row is for Tsukuba data (TK), and the bottom row is for Ascension Island data (AI). The colours in the plots are consistent with the rest of this paper in indicating the spectroscopic database. The units for all axes are indicated in the titles.

Fig C3 qualitatively indicates significant sensitivity to a methane profile shape perturbation, the linear regression statistics of Fig. C3 are shown in Fig C4, including slope, intercept, coefficient of determination and standard deviation.

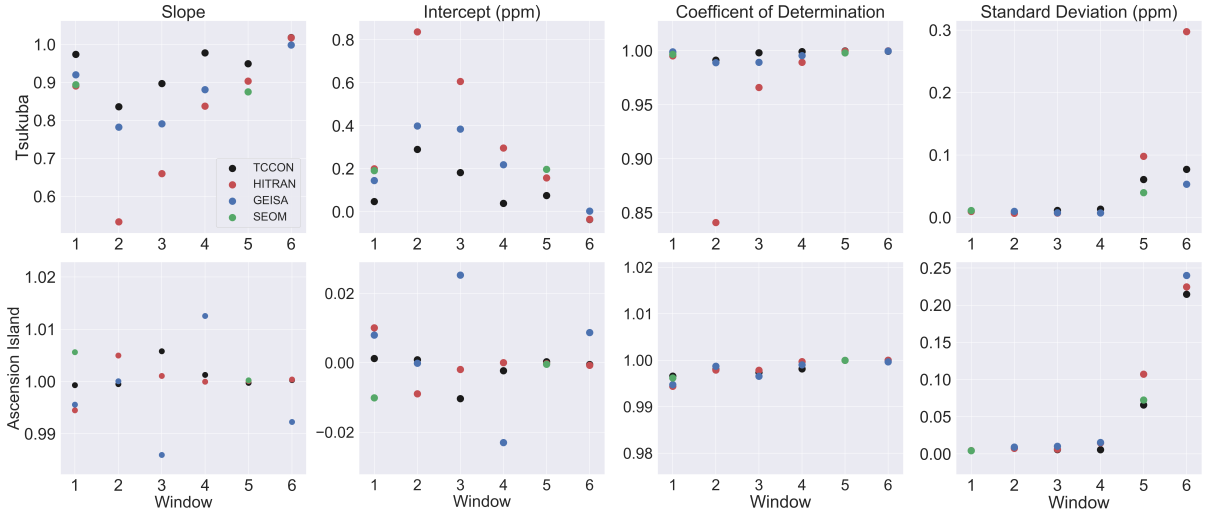

Figure C4. Plot indicating the linear statistical relationship between the perturbed and unperturbed $^{12}CH_4$ and $^{13}CH_4$ DMFs indicated in Fig C3 for the methane profile shape case. The x-axis for all plots indicates the retrieval window under consideration. The first column shows the values for the linear slope, the second column is the linear intercept, the third column is the coefficient of determination and the fourth column is the standard deviation. The first row indicates retrievals from Tsukuba and the second row shows retrievals from Ascension island. The colours in the plots are consistent with the rest of this paper in indicating the spectroscopic database.

Figure C4 indicates that Tsukuba retrievals were more sensitive to a change in profile shape than Ascension island, most likely because there is a more significant shift in the Tsukuba spring-summer profile, as opposed to the summer-autumn profile for Ascension island, where there are no seasons. Interestingly the HITRAN2016 retrievals are the most affected in the Tsukuba case, but there is no such clear pattern in Ascension island. Based on the results in Fig C4, we can assume that the magnitude of the biases specified in Table C2 will be as large (if not larger) for the Tsukuba July 2016 case, but no more significant than the results shown in Table C1 for the Ascension island cases.

C3 Water Vapour

An analysis on the impact of inserting a 10% water vapour profile shift error into the a priori information is included in this sub-appendix. Table C3 below allows for direct comparison with Table 5 of the impact of this shift.

Table C3. Statistics as Table 5 for the water profile profile shift case identified in sect. 2.4. Data is for April 2016 Tsukuba retrievals.

Window	1 ($^{12}CH_4$)	2 ($^{12}CH_4$)	3 ($^{12}CH_4$)	4 ($^{12}CH_4$)	5 ($^{13}CH_4$)	6 ($^{13}CH_4$)
σ_{window} (ppb)	9.02	17.4	22.5	12.9	0.556	1.65
Database			TCCON	HITRAN	GEISA	SEOM-IAS
$\sigma_{inter-window}$ $^{12}CH_4$ (ppb)			16.5	20.0	9.15	N/A
$\sigma_{inter-window}$ $^{13}CH_4$ (ppb)			1.09	0.406	N/A	N/A

Database	HITRAN	GEISA	SEOM-IAS
bias (ppb; window 1)	5.36	8.92	15.1
bias (ppb; window 2)	4.67	37.9	N/A
bias (ppb; window 3)	8.41	42.4	N/A
bias (ppb; window 4)	22.4	28.9	N/A
bias (ppb; window 5)	1.15	N/A	0.0191
bias (ppb; window 6)	0.410	3.59	N/A

Further analysis is below, showing the linear relationship between the original standard retrievals, and the perturbed retrievals. All Tsukuba and Ascension island retrievals considered in this study are included in these figures.

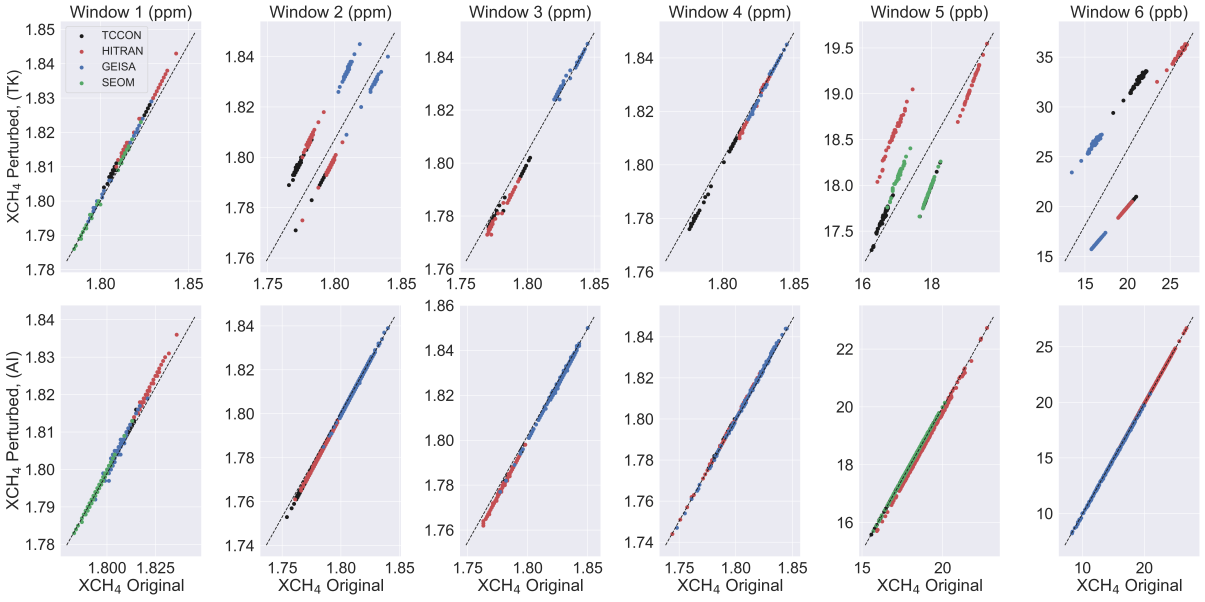

Figure C5. Series of scatter plots showing unperturbed retrieved DMFs $^{12}CH_4$ and $^{13}CH_4$ from the cases indicated in sect. 3.3 and Appendix B, against these cases when perturbed by a change to the a priori water vapour profile. Each column indicates the window under consideration, the top row is for Tsukuba data (TK), and the bottom row is for Ascension Island data (AI). The colours in the plots are consistent with the rest of this paper in indicating the spectroscopic database. The units for all axes are indicated in the titles.

Figure C5 shows that Tsukuba is far more sensitive to errors in the a priori water vapour column in some spectral windows than Ascension island. We note that the conditions for Tsukuba site in July of 2016 (indicated in Table D1) show very high levels of water vapour, which is a possible cause for this apparent sensitivity. The linear regression statistics shown in Fig. C6 below explore these differences in more detail.

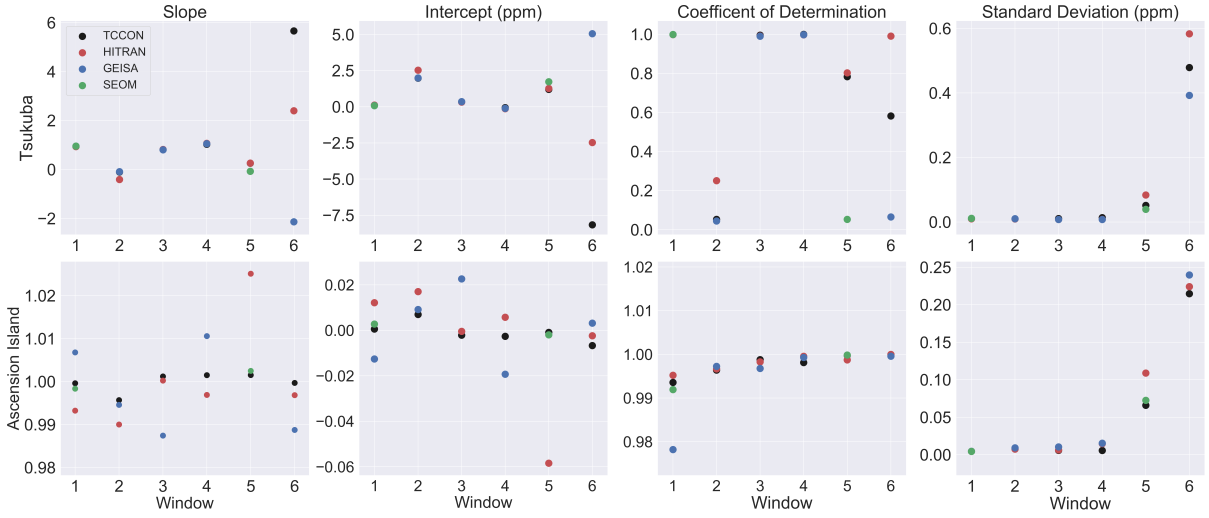

Figure C6. Plot indicating the linear statistical relationship between the perturbed and unperturbed $^{12}CH_4$ and $^{13}CH_4$ DMFs indicated in Fig C3 for the water vapour profile shift case. The x-axis for all plots indicates the retrieval window under consideration. The first column shows the values for the linear slope, the second column is the linear intercept, the third column is the coefficient of determination and the fourth column is the standard deviation. The first row indicates retrievals from Tsukuba and the second row shows retrievals from Ascension island. The colours in the plots are consistent with the rest of this paper in indicating the spectroscopic database.

Figure C6 shows some significant sensitivities to water vapour uncertainty, especially for retrievals from Tsukuba in window 2 for all spectroscopic databases, where the intercept value of 2.5 ppm is many times higher than any of the other cases shown in Fig. C6. We note that the values indicated in Table C3 are not significantly different from those in Table 5, suggesting that the majority of the errors occur in the July Tsukuba retrievals. The statistics for the Ascension island retrievals show similar values to those for the methane profile shift sensitivities, shown in Fig. C2, indicating lower sensitivity to water vapour uncertainty. Ascension island retains a consistent year round humidity due to its location; conversely Tsukuba has a wide range of seasons and therefore highly variable humidity, indicated in Table D1. The implication of these results is that a priori water vapour uncertainty only has a significant impact in high humidity environments.

C4 Pressure

An analysis on the impact of inserting a 2% pressure profile shift error into the parameter information is included in this sub-appendix. Table C4 below allows for direct comparison with Table 5 of the impact of this shift.

Table C4. Statistics as Table 5 for the pressure profile shift case identified in sect. 2.4. Data is for April 2016 Tsukuba retrievals.

Window	1 ($^{12}CH_4$)	2 ($^{12}CH_4$)	3 ($^{12}CH_4$)	4 ($^{12}CH_4$)	5 ($^{13}CH_4$)	6 ($^{13}CH_4$)
σ_{window} (ppb)	9.02	17.64	22.7	12.9	0.593	1.69
Database			TCCON	HITRAN	GEISA	SEOM-IAS
$\sigma_{inter-window}$ $^{12}CH_4$ (ppb)			15.1	18.5	10.7	N/A
$\sigma_{inter-window}$ $^{13}CH_4$ (ppb)			1.10	0.383	N/A	N/A

Database	HITRAN	GEISA	SEOM-IAS
bias (ppb; window 1)	5.44	8.95	15.1
bias (ppb; window 2)	4.87	38.5	N/A
bias (ppb; window 3)	8.36	42.9	N/A
bias (ppb; window 4)	22.5	29.1	N/A
bias (ppb; window 5)	1.23	N/A	0.0191
bias (ppb; window 6)	0.426	3.68	N/A

Further analysis is below, showing the linear relationship between the original standard retrievals, and the perturbed retrievals for all retrievals considered in this study.

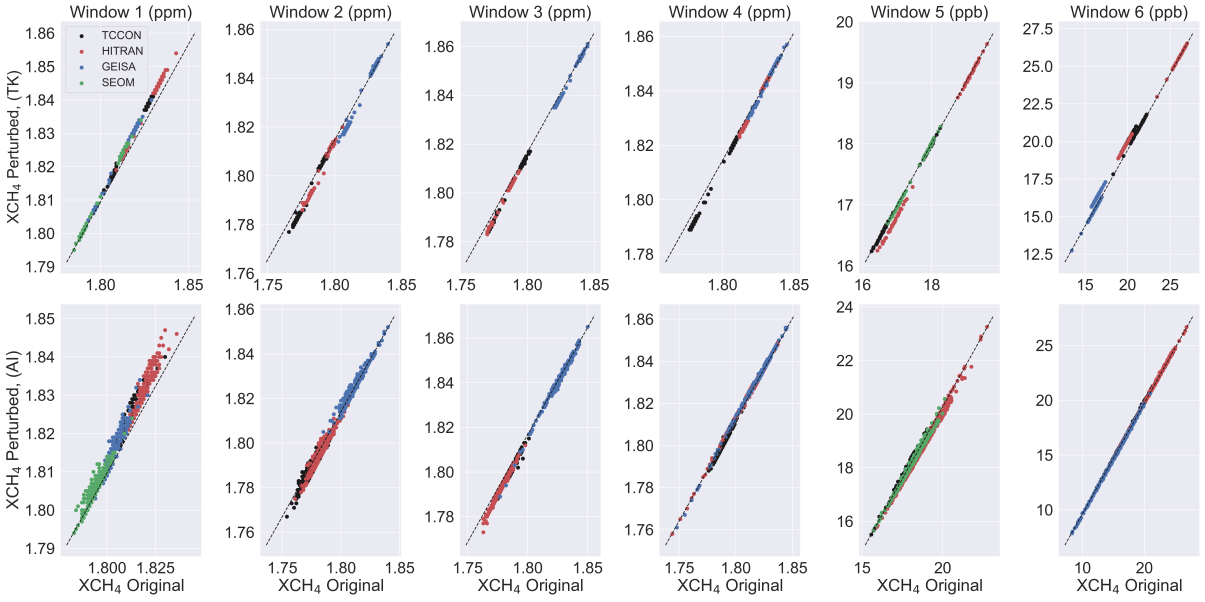

Figure C7. Series of scatter plots indicating the differences between retrieved values of $^{12}CH_4$ and $^{13}CH_4$ DMFs from the standard cases shown in sect. 3.3 and when a 2 % pressure shift is applied to the a priori atmosphere. Each column indicates the window under consideration, the top row is for Tsukuba data (TK), and the bottom row is for Ascension Island data (AI). The colours in the plots are consistent with the rest of this paper in indicating the spectroscopic database.

The results shown in Fig. C7 qualitatively indicate that there is significant dependency on the accurate knowledge of the pressure profile, which varies between the TCCON sites. Figure C8 below quantitatively explores the variations though linear regression statistics.

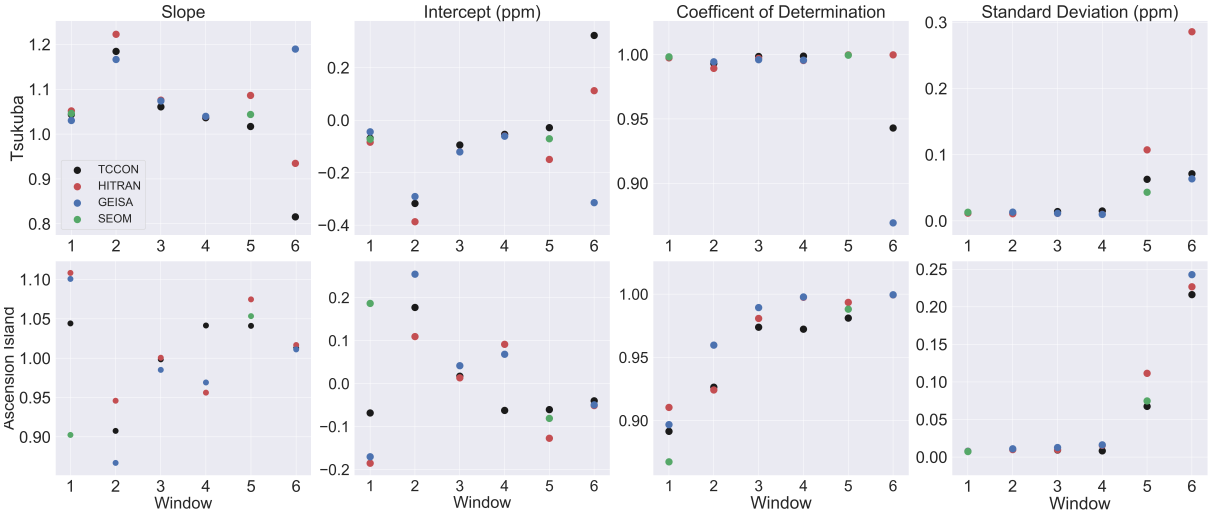

Figure C8. Plot indicating the linear statistical relationship between the standard retrievals from sect 3.3 and the perturbed pressure column retrievals. The x-axis for all plots indicates the retrieval window under consideration. The first column shows the values for the linear slope, the second column is the linear intercept, the third column is the coefficient of determination and the fourth column is the standard deviation. The first row indicates retrievals from Tsukuba and the second row shows retrievals from Ascension island. The colours in the plots are consistent with the rest of this paper in indicating the spectroscopic database.

Figure C8 shows that the sensitivity of retrieved $^{12}CH_4$ and $^{13}CH_4$ DMFs to a systematic bias in the pressure profile varies depending on the spectroscopic database, and the window. The fact that different spectroscopic databases and different windows react differently to pressure profile error is not surprising, the significance of the differences in all cases is. For the $^{12}CH_4$ cases (windows 1-4), window 2 typically shows the most sensitivity while for the $^{13}CH_4$ cases (windows 5-6), window 6 shows the most sensitivity. Interestingly, the results from Ascension island suggest greater insensitivity to the pressure error, but this could be attributed to a greater number of measurements available for this analysis. Comparisons of Table C4 with Tables C2 and 5 suggest the pressure column error has a greater impact on the bias against TCCON database retrievals, but the overall window and inter-window deviation is more significant with methane profile shape errors.

C5 Temperature

An analysis on the impact of inserting a 2 K temperature profile shift error into the parameter information is included in this sub-appendix. Table C5 below allows for direct comparison with Table 5 of the impact of this shift.

Table C5. Statistics as Table 5 for the temperature profile shift case identified in sect. 2.4. Data is for April 2016 Tsukuba retrievals.

Window	1 ($^{12}CH_4$)	2 ($^{12}CH_4$)	3 ($^{12}CH_4$)	4 ($^{12}CH_4$)	5 ($^{13}CH_4$)	6 ($^{13}CH_4$)
σ_{window} (ppb)	9.05	17.8	22.5	13.2	0.634	1.62
Database			TCCON	HITRAN	GEISA	SEOM-IAS
$\sigma_{inter-window}$ $^{12}CH_4$ (ppb)			17.5	20.8	8.4	N/A
$\sigma_{inter-window}$ $^{13}CH_4$ (ppb)			0.539	0.442	N/A	N/A

Database	HITRAN	GEISA	SEOM-IAS
bias (ppb; window 1)	5.46	8.87	15.2
bias (ppb; window 2)	5.69	39.1	N/A
bias (ppb; window 3)	8.08	42.6	N/A
bias (ppb; window 4)	22.9	29.6	N/A
bias (ppb; window 5)	1.29	N/A	0.0464
bias (ppb; window 6)	0.260	3.46	N/A

Further analysis is below, showing the linear relationship between the original standard retrievals, and the perturbed retrievals for all retrievals considered in this study.

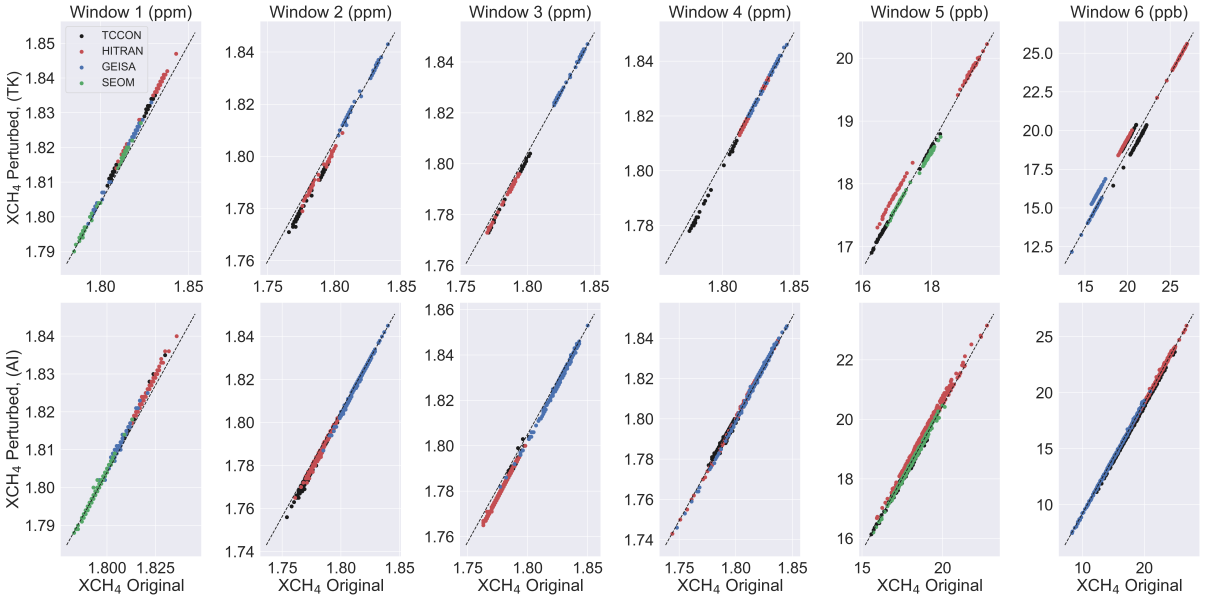

Figure C9. Series of scatter plots indicating the differences between retrieved values of $^{12}CH_4$ and $^{13}CH_4$ DMFs from the standard cases shown in sect. 3.3 and when a 2 K temperature shift is applied to the a priori atmosphere. Each column indicates the window under consideration, the top row is for Tsukuba data (TK), and the bottom row is for Ascension Island data (AI). The colours in the plots are consistent with the rest of this paper in indicating the spectroscopic database.

Figure C9 qualitatively shows adding a 2 K temperature bias into the parameter profile has a notable impact on the retrievals of $^{12}CH_4$ and $^{13}CH_4$ DMFs, especially windows 2 and 6. This is explored quantitatively in Figure C10.

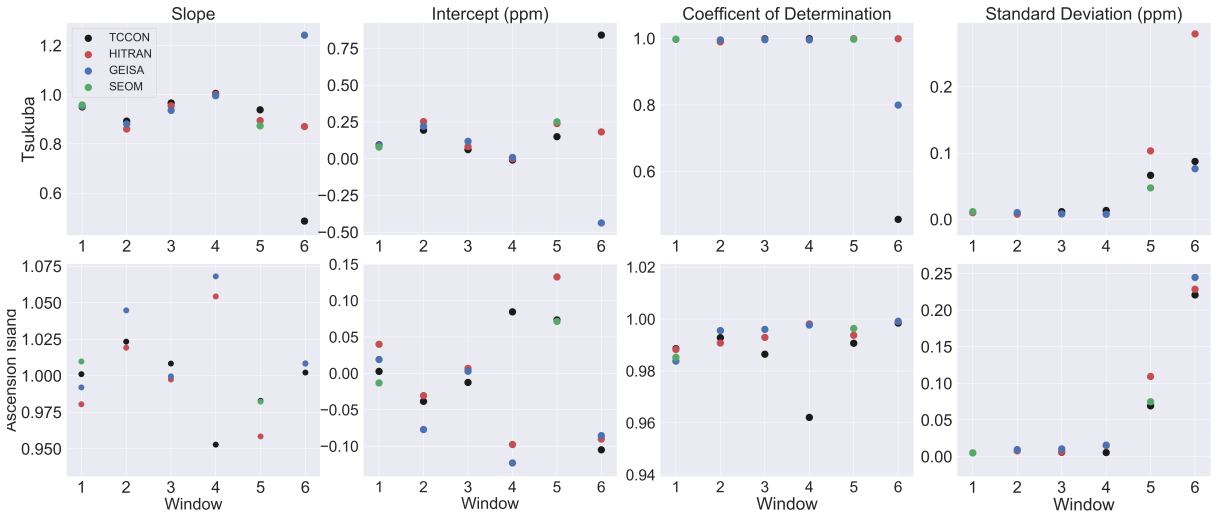

Figure C10. Plot indicating the linear statistical relationship between the standard retrievals from sect 3.3 and the perturbed temperature column retrievals. The x-axis for all plots indicates the retrieval window under consideration. The first column shows the values for the linear slope, the second column is the linear intercept, the third column is the coefficient of determination and the fourth column is the standard deviation. The first row indicates retrievals from Tsukuba and the second row shows retrievals from Ascension island. The colours in the plots are consistent with the rest of this paper in indicating the spectroscopic database.

The statistics indicated in Fig. C10 show a significant sensitivity to temperature biases, particularly at Tsukuba. Windows 2 and 4 show the most sensitivity in $^{12}CH_4$ DMFs, and window 6 shows the most for $^{13}CH_4$ DMFs. There is limited deviation between the spectroscopic databases in terms of sensitivity for each window, except for window 4 which shows more variability in this regards. The scale of these statistics is not as significant as those indicated in Figs C4 and C8 for methane profile and pressure profile errors respectively. Comparing the results from Table C5 with Table C4 and Table 5, it is possible to see that window deviation is similar in all cases, but the inter-window deviation is larger in the pressure profile errors case, but the biases tend to be larger in the temperature error case. Figures C7 and C8 seem to suggest larger errors for Ascension island than in Figures C9 and C10. These results suggest that retrievals of $^{12}CH_4$ DMFs and especially $^{13}CH_4$ DMFs are sensitive to temperature errors, and they depend on location and season significantly.

Appendix D: Additional data

Table D1. Daily ranges of a priori and measured surface temperatures, and averaged H_2O DMFs from both TCCON sites.

	A priori surface temperature (°C)	Site measured temperature (°C)	H_2O (average)	H_2O standard deviation	SZA range (°)
Tsukuba (01/April/2016)	12.0	15.8-16.8	2069 ppm	47 ppm	34-43
Tsukuba (01/July/2016)	25.1	29.2-33.2	6896 ppm	70 ppm	13-26
Ascension Island (23/Aug/2016)	22.4	24-27.3	3752 ppm	91 ppm	19-81
Ascension Island (01/Oct/2016)	22	24.3-25.9	4345 ppm	83 ppm	7-75

Water vapour retrievals are taken from the 4565 cm^{-1} spectral window.

Author contributions. DGF provided the Ascension Island TCCON data, IM provided the Ascension Island TCCON data. EM devised and performed the study, analysed the data and wrote the paper. BV consulted on the interpretation of the results. All authors reviewed the paper.

Competing interests. BV is an associate editor for the joint (AMT/ACP) special issue "TROPOMI on Sentinel-5 Precursor: first year in operation". DGF is an associate editor for AMT.

Acknowledgements. This study has been performed in the framework of the postdoctoral Research Fellowship program of the European Space Agency (ESA). The GGG2014 retrieval environment was developed at the California institute of Technology (Caltech), and is available at https://tccon-wiki.caltech.edu. Thanks to Geoff Toon at Caltech for providing advice on the use of GGG2014. HITRAN2016 is available at https://hitran.org/, GEISA2015 is available from http://ara.abct.lmd.polytechnique.fr/index.php?page=geisa-2. The SEOM-IAS database is available at https://www.wdc.dlr.de/seom-ias/. The TCCON line list is described in the GGG documentation. The Ascension Island TCCON station has been supported by ESA under grant 3-14737 and by the German Bundesministerium für Wirtschaft und Energie (BMWi) under grants 50EE1711C and 50EE1711E. The TCCON sites at Tsukuba is supported in part by the GOSAT series project. Thanks to Anu Dudhia at Oxford University for the Fortran routine to convert the GEISA line structure into a HITRAN line structure.

References

An, X., Caswell, A. W., and Sanders, S. T.: Quantifying the temperature sensitivity of practical spectra using a new spectroscopic quantity: Frequency-dependent lower-state energy, Journal of Quantitative Spectroscopy and Radiative Transfer, 112, 779–785, https://doi.org/10.1016/j.jqsrt.2010.10.014, https://www.sciencedirect.com/science/article/pii/S0022407310004000?via{%}3Dihub, 2011.

Armante, R., Scott, N., Crevoisier, C., Capelle, V., Crepeau, L., Jacquinet, N., and Chédin, A.: Evaluation of spectroscopic databases through radiative transfer simulations compared to observations. Application to the validation of GEISA 2015 with IASI and TCCON, Journal of Molecular Spectroscopy, 327, 180–192, https://doi.org/10.1016/j.jms.2016.04.004, https://www.sciencedirect.com/science/article/abs/pii/S002228521630056X?via{%}3Dihub, 2016.

Bernath, P. F., McElroy, C. T., Abrams, M. C., Boone, C. D., Butler, M., Camy-Peyret, C., Carleer, M., Clerbaux, C., Coheur, P., Colin, R., DeCola, P., DeMazière, M., Drummond, J. R., Dufour, D., Evans, W. F. J., Fast, H., Fussen, D., Gilbert, K., Jennings, D. E., Llewellyn, E. J., Lowe, R. P., Mahieu, E., McConnell, J. C., McHugh, M., McLeod, S. D., Michaud, R., Midwinter, C., Nassar, R., Nichitiu, F., Nowlan, C., Rinsland, C. P., Rochon, Y. J., Rowlands, N., Semeniuk, K., Simon, P., Skelton, R., Sloan, J. J., Soucy, M., Strong, K., Tremblay, P., Turnbull, D., Walker, K. A., Walkty, I., Wardle, D. A., Wehrle, V., Zander, R., and Zou, J.: Atmospheric Chemistry Experiment (ACE): Mission overview, Geophysical Research Letters, 32, L15S01, https://doi.org/10.1029/2005GL022386, http://doi.wiley.com/10.1029/2005GL022386, 2005.

Birk, M., Wagner, G., Loos, J., Mondelain, D., and Campargue, A.: ESA SEOM-IAS – Spectroscopic parameters database 2.3 μm region, https://doi.org/10.5281/ZENODO.1009126, https://zenodo.org/record/1009126, 2017.

Bovensmann, H., Burrows, J. P., Buchwitz, M., Frerick, J., Noël, S., Rozanov, V. V., Chance, K. V., and Goede, A. P. H.: SCIAMACHY: Mission Objectives and Measurement Modes, Journal of the Atmospheric Sciences, 56, 127–150, https://doi.org/10.1175/1520-0469(1999)056<0127:SMOAMM>2.0.CO;2, http://journals.ametsoc.org/doi/pdf/10.1175/1520-0469{%}281999{%}29056{%}3C0127{%}3ASMOAMM{%}3E2.0.CO{%}3B2http://journals.ametsoc.org/doi/abs/10.1175/1520-0469{%}281999{%}29056{%}3C0127{%}3ASMOAMM{%}3E2.0.CO{%}3B2, 1999.

Buzan, E. M., Beale, C. A., Boone, C. D., and Bernath, P. F.: Global stratospheric measurements of the isotopologues of methane from the Atmospheric Chemistry Experiment Fourier transform spectrometer, Atmos. Meas. Tech, 9, 1095–1111, https://doi.org/10.5194/amt-9-1095-2016, www.atmos-meas-tech.net/9/1095/2016/, 2016.

Checa-Garcia, R., Landgraf, J., Galli, A., Hase, F., Velazco, V. A., Tran, H., Boudon, V., Alkemade, F., and Butz, A.: Mapping spectroscopic uncertainties into prospective methane retrieval errors from Sentinel-5 and its precursor, Atmospheric Measurement Techniques, 8, 3617–3629, https://doi.org/10.5194/amt-8-3617-2015, www.atmos-meas-tech.net/8/3617/2015/, 2015.

Crisp, D., Fisher, B. M., O 'dell, C., Frankenberg, C., Basilio, R., Bösch, H., Brown, L. R., Castano, R., Connor, B., Deutscher, N. M., Eldering, A., Griffith, D., Gunson, M., Kuze, A., Mandrake, L., Mcduffie, J., Messerschmidt, J., Miller, C. E., Morino, I., Natraj, V., Notholt, J., O 'brien, D. M., Oyafuso, F., Polonsky, I., Robinson, J., Salawitch, R., Sherlock, V., Smyth, M., Suto, H., Taylor, T. E., Thompson, D. R., Wennberg, P. O., Wunch, D., and Yung, Y. L.: The ACOS CO 2 retrieval algorithm – Part II: Global X CO 2 data characterization, Atmos. Meas. Tech, 5, 687–707, https://doi.org/10.5194/amt-5-687-2012, www.atmos-meas-tech.net/5/687/2012/, 2012.

Drummond, J. R. and Mand, G. S.: The measurements of pollution in the troposphere (MOPITT) instrument: Overall performance and calibration requirements, Journal of Atmospheric and Oceanic Technology, 13, 314–

320, https://doi.org/10.1175/1520-0426(1996)013<0314:TMOPIT>2.0.CO;2, http://journals.ametsoc.org/doi/abs/10.1175/1520-0426{%}281996{%}29013{%}3C0314{%}3ATMOPIT{%}3E2.0.CO{%}3B2, 1996.

Fisher, R. E., France, J. L., Lowry, D., Lanoisellé, M., Brownlow, R., Pyle, J. A., Cain, M., Warwick, N., Skiba, U. M., Drewer, J., Dinsmore, K. J., Leeson, S. R., Bauguitte, S. J.-B., Wellpott, A., O'Shea, S. J., Allen, G., Gallagher, M. W., Pitt, J., Percival, C. J., Bower, K., George, C., Hayman, G. D., Aalto, T., Lohila, A., Aurela, M., Laurila, T., Crill, P. M., McCalley, C. K., and Nisbet, E. G.: Measurement of the 13C isotopic signature of methane emissions from northern European wetlands, Global Biogeochemical Cycles, 31, 605–623, https://doi.org/10.1002/2016GB005504, http://doi.wiley.com/10.1002/2016GB005504, 2017.

Galli, A., Butz, A., Scheepmaker, R. A., Hasekamp, O., Landgraf, J., Tol, P., Wunch, D., Deutscher, N. M., Toon, G. C., Wennberg, P. O., Griffith, D. W., and AbenI.: CH4, CO, and H2O spectroscopy for the Sentinel-5 Precursor mission: An assessment with the Total Carbon Column Observing Network measurements, Atmospheric Measurement Techniques, 5, 1387–1398, https://doi.org/10.5194/amt-5-1387-2012, http://www.atmos-meas-tech.net/5/1387/2012/, 2012.

Gordon, I., Rothman, L., Hill, C., Kochanov, R., Tan, Y., Bernath, P., Birk, M., Boudon, V., Campargue, A., Chance, K., Drouin, B., Flaud, J.-M., Gamache, R., Hodges, J., Jacquemart, D., Perevalov, V., Perrin, A., Shine, K., Smith, M.-A., Tennyson, J., Toon, G., Tran, H., Tyuterev, V., Barbe, A., Császár, A., Devi, V., Furtenbacher, T., Harrison, J., Hartmann, J.-M., Jolly, A., Johnson, T., Karman, T., Kleiner, I., Kyuberis, A., Loos, J., Lyulin, O., Massie, S., Mikhailenko, S., Moazzen-Ahmadi, N., Müller, H., Naumenko, O., Nikitin, A., Polyansky, O., Rey, M., Rotger, M., Sharpe, S., Sung, K., Starikova, E., Tashkun, S., Auwera, J. V., Wagner, G., Wilzewski, J., Wcisło, P., Yu, S., and Zak, E.: The HITRAN2016 Molecular Spectroscopic Database, Journal of Quantitative Spectroscopy and Radiative Transfer, https://doi.org/10.1016/j.jqsrt.2017.06.038, http://www.sciencedirect.com/science/article/pii/S0022407317301073, 2017.

Hu, H., Hasekamp, O., Butz, A., Galli, A., Landgraf, J., Aan De Brugh, J., Borsdorff, T., Scheepmaker, R., and Aben, I.: The operational methane retrieval algorithm for TROPOMI, Atmos. Meas. Tech, 9, 5423–5440, https://doi.org/10.5194/amt-9-5423-2016, www.atmos-meas-tech.net/9/5423/2016/, 2016.

Ingmann, P., Veihelmann, B., Langen, J., Lamarre, D., Stark, H., and Courrèges-Lacoste, G. B.: Requirements for the GMES Atmosphere Service and ESA's implementation concept: Sentinels-4/-5 and -5p, Remote Sensing of Environment, 120, 58–69, https://doi.org/10.1016/J.RSE.2012.01.023, https://www.sciencedirect.com/science/article/pii/S0034425712000673, 2012.

IPCC: Fifth Assessment Report - Impacts, Adaptation and Vulnerability, http://www.ipcc.ch/report/ar5/wg2/, 2014.

Jacquinet-Husson, N., Armante, R., Scott, N. A., Chédin, A., Crépeau, L., Boutammine, C., Bouhdaoui, A., Crevoisier, C., Capelle, V., Boonne, C., Poulet-Crovisier, N., Barbe, A., Chris Benner, D., Boudon, V., Brown, L. R., Buldyreva, J., Campargue, A., Coudert, L. H., Devi, V. M., Down, M. J., Drouin, B. J., Fayt, A., Fittschen, C., Flaud, J. M., Gamache, R. R., Harrison, J. J., Hill, C., Hodnebrog, Hu, S. M., Jacquemart, D., Jolly, A., Jiménez, E., Lavrentieva, N. N., Liu, A. W., Lodi, L., Lyulin, O. M., Massie, S. T., Mikhailenko, S., Müller, H. S., Naumenko, O. V., Nikitin, A., Nielsen, C. J., Orphal, J., Perevalov, V. I., Perrin, A., Polovtseva, E., Predoi-Cross, A., Rotger, M., Ruth, A. A., Yu, S. S., Sung, K., Tashkun, S. A., Tennyson, J., Tyuterev, V. G., Vander Auwera, J., Voronin, B. A., and Makie, A.: The 2015 edition of the GEISA spectroscopic database, Journal of Molecular Spectroscopy, 327, 31–72, https://doi.org/10.1016/j.jms.2016.06.007, https://www.sciencedirect.com/science/article/pii/S0022285216301011, 2016.

Kirschke, S., Bousquet, P., Ciais, P., Saunois, M., Canadell, J. G., Dlugokencky, E. J., Bergamaschi, P., Bergmann, D., Blake, D. R., Bruhwiler, L., Cameron-Smith, P., Castaldi, S., Chevallier, F., Feng, L., Fraser, A., Heimann, M., Hodson, E. L., Houweling, S., Josse, B., Fraser, P. J., Krummel, P. B., Lamarque, J. F., Langenfelds, R. L., Le Quéré, C., Naik, V., O'doherty, S., Palmer, P. I., Pison, I., Plummer, D., Poulter, B., Prinn, R. G., Rigby, M., Ringeval, B., Santini, M., Schmidt, M., Shindell, D. T., Simpson, I. J., Spahni, R., Steele, L. P., Strode, S. A., Sudo, K., Szopa, S., Van Der Werf, G. R., Voulgarakis, A., Van Weele, M., Weiss, R. F., Williams, J. E., and Zeng, G.: Three decades

of global methane sources and sinks, https://doi.org/10.1038/ngeo1955, https://www.nature.com/ngeo/journal/v6/n10/pdf/ngeo1955.pdf, 2013.

Kuze, A., Suto, H., Nakajima, M., and Hamazaki, T.: Thermal and near infrared sensor for carbon observation Fourier-transform spectrometer on the Greenhouse Gases Observing Satellite for greenhouse gases monitoring, Applied Optics, 48, 6716, https://doi.org/10.1364/AO.48.006716, https://www.osapublishing.org/abstract.cfm?URI=ao-48-35-6716, 2009.

Malina, E., Yoshida, Y., Matsunaga, T., and Muller, J. P.: Information content analysis: The potential for methane isotopologue retrieval from GOSAT-2, Atmospheric Measurement Techniques, 11, 1159–1179, https://doi.org/10.5194/amt-11-1159-2018, https://www.atmos-meas-tech.net/11/1159/2018/amt-11-1159-2018.pdf, 2018.

Malina, E., Hu, H., Landgraf, J., and Veihelmann, B.: A study of synthetic 13 CH 4 retrievals from TROPOMI and Sentinel-5/UVNS, Atmos. Meas. Tech, 12, 6273–6301, https://doi.org/10.5194/amt-12-6273-2019, https://doi.org/10.5194/amt-12-6273-2019, 2019.

Mcnorton, J., Chipperfield, M. P., Gloor, M., Wilson, C., Feng, W., Hayman, G. D., Rigby, M., Krummel, P. B., O 'doherty, S., Prinn, R. G., Weiss, R. F., Young, D., Dlugokencky, E., and Montzka, S. A.: Role of OH variability in the stalling of the global atmospheric CH 4 growth rate from 1999 to 2006, Atmos. Chem. Phys, 16, 7943–7956, https://doi.org/10.5194/acp-16-7943-2016, www.atmos-chem-phys.net/16/7943/2016/, 2016.

Mendonca, J., Strong, K., Sung, K., Devi, V. M., Toon, G. C., Wunch, D., and Franklin, J. E.: Using high-resolution laboratory and ground-based solar spectra to assess CH4 absorption coefficient calculations, Journal of Quantitative Spectroscopy and Radiative Transfer, 190, 48–59, https://doi.org/10.1016/j.jqsrt.2016.12.013, 2017.

Ngo, N. H., Lisak, D., Tran, H., and Hartmann, J. M.: An isolated line-shape model to go beyond the Voigt profile in spectroscopic databases and radiative transfer codes, Journal of Quantitative Spectroscopy and Radiative Transfer, 129, 89–100, https://doi.org/10.1016/j.jqsrt.2013.05.034, https://www.sciencedirect.com/science/article/pii/S0022407313002422, 2013.

Nisbet, E. G., Dlugokencky, E. J., Manning, M. R., Lowry, D., Fisher, R. E., France, J. L., Michel, S. E., Miller, J. B., White, J. W. C., Vaughn, B., Bousquet, P., Pyle, J. A., Warwick, N. J., Cain, M., Brownlow, R., Zazzeri, G., Lanoisellé, M., Manning, A. C., Gloor, E., Worthy, D. E. J., Brunke, E.-G., Labuschagne, C., Wolff, E. W., and Ganesan, A. L.: Rising atmospheric methane: 2007-2014 growth and isotopic shift, Global Biogeochemical Cycles, 30, 1356–1370, https://doi.org/10.1002/2016GB005406, http://doi.wiley.com/10.1002/2016GB005406, 2016.

Parker, R. J., Boesch, H., Byckling, K., Webb, A. J., Palmer, P. I., Feng, L., Bergamaschi, P., Chevallier, F., Notholt, J., Deutscher, N., Warneke, T., Hase, F., Sussmann, R., Kawakami, S., Kivi, R., Griffith, D. W. T., and Velazco, V.: Assessing 5 years of GOSAT Proxy XCH 4 data and associated uncertainties, Atmos. Meas. Tech, 8, 4785–4801, https://doi.org/10.5194/amt-8-4785-2015, www.atmos-meas-tech.net/8/4785/2015/, 2015.

Rahpoe, N., Von Savigny, C., Weber, M., Rozanov, A. V., Bovensmann, H., and Burrows, J. P.: Atmospheric Measurement Techniques Error budget analysis of SCIAMACHY limb ozone profile retrievals using the SCIATRAN model, Atmos. Meas. Tech, 6, 2825–2837, https://doi.org/10.5194/amt-6-2825-2013, www.atmos-meas-tech.net/6/2825/2013/, 2013.

Rella, C. W., Hoffnagle, J., He, Y., and Tajima, S.: Local-and regional-scale measurements of CH 4 , δ 13 CH 4 , and C 2 H 6 in the Uintah Basin using a mobile stable isotope analyzer, Atmos. Meas. Tech, 8, 4539–4559, https://doi.org/10.5194/amt-8-4539-2015, www.atmos-meas-tech.net/8/4539/2015/, 2015.

Rigby, M., Montzka, S. A., Prinn, R. G., White, J. W. C., Young, D., O'Doherty, S., Lunt, M. F., Ganesan, A. L., Manning, A. J., Simmonds, P. G., Salameh, P. K., Harth, C. M., Mühle, J., Weiss, R. F., Fraser, P. J., Steele, L. P., Krummel, P. B., McCulloch, A., and Park, S.: Role of atmospheric oxidation in recent methane growth., Proceedings of the National Academy of Sciences of the United States of America,

114, 5373–5377, https://doi.org/10.1073/pnas.1616426114, http://www.ncbi.nlm.nih.gov/pubmed/28416657http://www.pubmedcentral.nih.gov/articlerender.fcgi?artid=PMC5448198, 2017.

Röckmann, T., Brass, M., Borchers, R., and Engel, A.: The isotopic composition of methane in the stratosphere: High-altitude balloon sample measurements, Atmospheric Chemistry and Physics, 11, 13 287–13 304, https://doi.org/10.5194/acp-11-13287-2011, www.atmos-chem-phys.net/11/13287/2011/, 2011.

Rodgers, C. D.: Inverse Methods for Atmospheric Sounding - Theory and Practice, vol. 2, World Scientific, https://doi.org/10.1142/9789812813718, http://www.worldscientific.com/worldscibooks/10.1142/3171http://ebooks.worldscinet.com/ISBN/9789812813718/9789812813718.html, 2000.

Saunois, M., Stavert, A. R., Poulter, B., Bousquet, P., Canadell, J. G., Jackson, R. B., Raymond, P. A., Dlugokencky, E. J., Houweling, S., Patra, P. K., Ciais, P., Arora, V. K., Bastviken, D., Bergamaschi, P., Blake, D. R., Brailsford, G., Bruhwiler, L., Carlson, K. M., Carrol, M., Castaldi, S., Chandra, N., Crevoisier, C., Crill, P. M., Covey, K., Curry, C. L., Etiope, G., Frankenberg, C., Gedney, N., Hegglin, M. I., Höglund-Isakson, L., Hugelius, G., Ishizawa, M., Ito, A., Janssens-Maenhout, G., Jensen, K. M., Joos, F., Kleinen, T., Krummel, P. B., Langenfelds, R. L., Laruelle, G. G., Liu, L., Machida, T., Maksyutov, S., McDonald, K. C., McNorton, J., Miller, P. A., Melton, J. R., Morino, I., Müller, J., Murgia-Flores, F., Naik, V., Niwa, Y., Noce, S., O'Doherty, S., Parker, R. J., Peng, C., Peng, S., Peters, G. P., Prigent, C., Prinn, R., Ramonet, M., Regnier, P., Riley, W. J., Rosentreter, J. A., Segers, A., Simpson, I. J., Shi, H., Smith, S. J., Steele, P. L., Thornton, B. F., Tian, H., Tohjima, Y., Tubiello, F. N., Tsuruta, A., Viovy, N., Voulgarakis, A., Weber, T. S., van Weele, M., van der Werf, G. R., Weiss, R. F., Worthy, D., Wunch, D., Yin, Y., Yoshida, Y., Zhang, W., Zhang, Z., Zhao, Y., Zheng, B., Zhu, Q., Zhu, Q., and Zhuang, Q.: The Global Methane Budget 2000-2017, Earth System Science Data Discussions, pp. 1–138, https://doi.org/10.5194/essd-2019-128, https://doi.org/10.5194/essd-2019-128, 2019.

Schneising, O., Buchwitz, M., Reuter, M., Bovensmann, H., Burrows, J. P., Borsdorff, T., Deutscher, N. M., Feist, D. G., Griffith, D. W. T., Hase, F., Hermans, C., Iraci, L. T., Kivi, R., Landgraf, J., Morino, I., Notholt, J., Petri, C., Pollard, D. F., Roche, S., Shiomi, K., Strong, K., Sussmann, R., Velazco, V. A., Warneke, T., and Wunch, D.: A scientific algorithm to simultaneously retrieve carbon monoxide and methane from TROPOMI onboard Sentinel-5 Precursor, Atmospheric Measurement Techniques Discussions, pp. 1–44, https://doi.org/10.5194/amt-2019-243, https://doi.org/10.5194/amt-2019-243https://www.atmos-meas-tech-discuss.net/amt-2019-243/, 2019.

Sherwood, O., Schwietzke, S., Arling, V., and Etiope, G.: Global Inventory of Fossil and Non-fossil Methane δ13C Source Signature Measurements for Improved Atmospheric Modeling, https://doi.org/10.15138/G37P4D, http://www.esrl.noaa.gov/gmd/ccgg/d13C-src-inv/, 2016.

TCCON: Using the cc option in GGG2014 - Tccon-wiki, https://tccon-wiki.caltech.edu/index.php?title=Software/GGG/Download/GGG{_}2014{_}Release{_}Notes/Using{_}the{_}cc{_}option{_}in{_}GGG2014{&}highlight=continuum+curvature, 2020.

Toon, G. C.: Atmospheric Line List for the 2014 TCCON Data Release, https://doi.org/10.14291/tccon.ggg2014.atm.R0/1221656, http://dx.doi.org/10.14291/tccon.ggg2014.atm.R0/1221656http://dx.doi.org/10.14291/tccon.ggg2014.solar.R0/1221658, 2015.

Tran, H., Ngo, N., and Hartmann, J.-M.: Efficient computation of some speed-dependent isolated line profiles, Journal of Quantitative Spectroscopy and Radiative Transfer, 129, 199–203, https://doi.org/10.1016/J.JQSRT.2013.06.015, https://www.sciencedirect.com/science/article/pii/S0022407313002598, 2013.

Veefkind, J. P., Aben, I., McMullan, K., Förster, H., de Vries, J., Otter, G., Claas, J., Eskes, H. J., de Haan, J. F., Kleipool, Q., van Weele, M., Hasekamp, O., Hoogeveen, R., Landgraf, J., Snel, R., Tol, P., Ingmann, P., Voors, R., Kruizinga, B., Vink, R., Visser, H., and Levelt,

P. F.: TROPOMI on the ESA Sentinel-5 Precursor: A GMES mission for global observations of the atmospheric composition for climate, air quality and ozone layer applications, Remote Sensing of Environment, 120, 70–83, https://doi.org/10.1016/j.rse.2011.09.027, 2012.

Weidmann, D., Hoffmann, A., Macleod, N., Middleton, K., Kurtz, J., Barraclough, S., and Griffin, D.: The Methane Isotopologues by Solar Occultation (MISO) Nanosatellite Mission: Spectral Channel Optimization and Early Performance Analysis, Remote Sensing, 9, 1073, https://doi.org/10.3390/rs9101073, http://www.mdpi.com/2072-4292/9/10/1073, 2017.

Wunch, D., Toon, G. C., Wennberg, P. O., Wofsy, S. C., Stephens, B. B., Fischer, M. L., Uchino, O., Abshire, J. B., Bernath, P., Biraud, S. C., Blavier, J.-F. L., Boone, C., Bowman, K. P., Browell, E. V., Campos, T., Connor, B. J., Daube, B. C., Deutscher, N. M., Diao, M., Elkins, J. W., Gerbig, C., Gottlieb, E., Griffith, D. W. T., and Hurst, D. F.: Calibration of the Total Carbon Column Observing Network using aircraft profile data, Atmos. Meas. Tech, 3, 1351–1362, https://doi.org/10.5194/amt-3-1351-2010, www.atmos-meas-tech.net/3/1351/2010/, 2010.

Wunch, D., Toon, G. C., Blavier, J.-F. L., Washenfelder, R. A., Notholt, J., Connor, B. J., Griffith, D. W. T., Sherlock, V., and Wennberg, P. O.: The Total Carbon Column Observing Network, Phil. Trans. R. Soc. A, 369, 2087–2112, https://doi.org/10.1098/rsta.2010.0240, http://rsta.royalsocietypublishing.org/content/roypta/369/1943/2087.full.pdf, 2011.

Wunch, D., Toon, G., Sherlock, V., Deutscher, N., Liu, C., Feist, D., and Wennberg, P.: The Total Carbon Column Observing Network's GGG2014 Data Version, Tech. rep., https://doi.org/10.14291/tccon.ggg2014.documentation.R0/1221662, ftp://tccon.ornl.gov/2014Public/documentation/tccon{_}ggg2014.pdf, 2015.

Yoshida, Y., Ota, Y., Eguchi, N., Kikuchi, N., Nobuta, K., Tran, H., Morino, I., and Yokota, T.: Retrieval algorithm for CO 2 and CH 4 column abundances from short-wavelength infrared spectral observations by the Greenhouse gases observing satellite, Atmos. Meas. Tech, 4, 717–734, https://doi.org/10.5194/amt-4-717-2011, www.atmos-meas-tech.net/4/717/2011/, 2011.

Zhou, M., Langerock, B., Sha, M. K., Kumps, N., Hermans, C., Petri, C., Warneke, T., Chen, H., Metzger, J. M., Kivi, R., Heikkinen, P., Ramonet, M., and De Mazière, M.: Retrieval of atmospheric CH4 vertical information from ground-based FTS near-infrared spectra, Atmospheric Measurement Techniques, 12, 6125–6141, https://doi.org/10.5194/amt-12-6125-2019, https://www.atmos-meas-tech.net/12/6125/2019/, 2019.